ALMA MATER STUDIORUM
UNIVERSITÀ DI BOLOGNA

FACOLTÀ DI SCIENZE MATEMATICHE FISICHE E NATURALI

Corso di laurea magistrale in BIOLOGIA MARINA

Modelling growth dynamics and toxin production in *Ostreopsis* cf. *ovata*

Relatore:

Prof.ssa Rossella Pistocchi

Presentata da:

Adriano Pinna

Correlatori:

Dott.ssa Laura Pezzolesi

Dott. Luca Polimene

(III sessione)

Anno Accademico 2012 / 2013

INDEX

1. INTRODUCTION

1.1 The toxic dinoflagellate *Ostreopsis ovata*

1.1.1 Geographical distribution, morphological description and ecology of O. ovata

The genus *Ostreopsis* Schmidt, together with the genus *Coolia* Meunier, composes the family of Ostreopsidaceae, order Gonyaulacales, class Dinophyceae, phylum Dinophyta.

Ostreopsis genus is actually represented by 9 species of marine dinoflagellates, some of which are toxic (condition here indicated with [t]): *O. siamensis* [t] Schmidt (1901), *O. ovata* [t] Fukuyo (1981), *O. lenticularis* [t] Fukuyo (1981), *O. heptagona* [t] Norris, Bomber and Balech (1985), *O. mascarenensis* [t] Quod (1994), *O. labens* [t] Faust and Morton (1995), *O. marinus* Faust (1999), *O. belizeanus* Faust (1999), and *O. caribbeanus* Faust (1999) (Penna et al., 2005).

The aforementioned toxicity of some species belonging to this genus, their ability to develop large blooms, and an apparent increase in their distribution range (at least for some species), make them an interesting subject of study (Rhodes, 2011).

The species of the genus *Ostreopsis*, as many other dinoflagellates, are mostly distinguished for morphological traits, like form and dimension of the cells, plates type and number, and incisions on these lasts. However, because of a quite high intra-specific morphological variability, and a relative similarity between some species, sometimes molecular analysis could be required to distinguish between them (Pin et al., 2001; Battocchi et al., 2010; Penna et al., 2012); moreover molecular studies could also give useful information about phylogeny and biogeography of the species.

Ostreopsis spp. dinoflagellates have a nearly worldwide **distribution** in tropical areas of the oceans, and are also diffused in some temperate waters (Japan, Southern Australia, New Zealand, Mediterranean Sea) (Fig. 1) where recently they have caused several blooms (Faust et al., 1996; Shears & Ross, 2009; Rhodes, 2011).

To date, in the Mediterranean Sea have been recovered only two species belonging to the *Ostreopsis* genus: *O.* cf. *siamensis* Schmidt in the 70s (Taylor, 1979) and *O.* cf. *ovata* Fukuyo in the 90s (Tognetto et al., 1995).

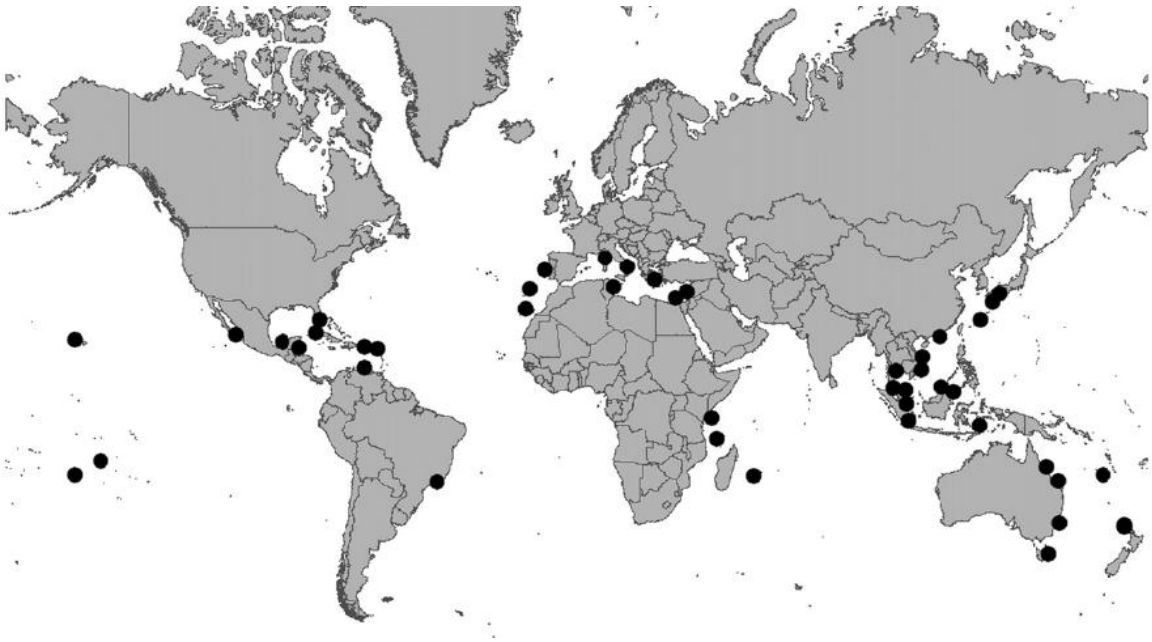

Figure 1. Distribution across the world of the dinoflagellates belonging to the *Ostreopsis* genus (from Rhodes, 2011).

An Adriatic ***Ostreopsis* cf. *ovata*** strain is the subject of this study.

In recent times this dinoflagellate has been studied quite extensively in many aspects by scientists [Vila et al., 2001; Turki, 2005; Ciminiello et al., 2006; Riobó et al., 2006; Guerrini et al., 2010; special issue on Ostreopsis in Toxicon, 57 (2001); and many others] because of its increasing diffusion along densely populated temperate coasts, coupled to its ability in producing toxins (see the following section 1.1.2 and 1.1.3).

O. cf. *ovata* is present in many tropical areas, and with regard to the Mediterranean Sea it has been found in high concentrations during the two last decades along the coasts of Spain (Penna et al., 2005; Bravo et al., 2012), France (Sechet et al., 2012; Cohu et al., 2013), Italy (Tognetto et al., 1995; Mangialajo et al., 2008; Totti et al., 2010), Croatia (Monti et al., 2007; Bravo et al., 2012), Greece (Aligizaki & Nikolaidis, 2006) and Tunisia (Turki, 2005; Sechet et al., 2012). It is still not clear if this alga has reached and colonized the Mediterranean Sea recently, transported from tropical seas via ballast-waters of ships, or if it was already present but at very low cell density, since bloom of this species were not recorded before the 90s. From some molecular studies, based on the LSU(D1/D2) - ITS - 5.8S rDNAs of some *Ostreopsis* spp. and *Coolia monotis* (considered as an outgroup reference) performed on several samples from different areas of the Mediterranean and eastern Atlantic coasts, resulted that *O.* cf. *ovata* has a single panmictic population for these areas, quite distinct from populations of the Indo-Pacific (Penna et al., 2010; Penna et al., 2012). This result leads to suppose that a well-structured Mediterranean/Eastern-Atlantic population was

already present for long time, therefore being not a recent colonization from tropical sea. Qualitative and quantitative molecular assays, as seen, can be extremely sensitive and could improve geographical distribution studies on *Ostreopsis* spp. in the future (Penna et al., 2007).

About **morphology**, *O. ovata* is a thecate dinoflagellate of medium size, with color ranging from ocher to dark brown: as the name suggests, this alga is oval to tear shaped, pointed to the ventral side, with an ephitheca which is equal in size to the hypotheca, both composed of thin and delicate thecal plates (Fig. 2). Although it was observed an high intra-specific morphometric variability, especially in clonal cultures (less in field samples), it has been possible to determine some distinguishing features of this species. In Penna et al. (2005) and Aligizaki & Nikolaidis (2006) cells of different *O.* cf. *ovata* strains were compared to cells of several strains of the most similar species, *O.* cf. *siamensis*: *O.* cf. *ovata* resulted to have a DV diameter ranging between 26 and 65 μm, a width from 13 to 57 μm, and an AP diameter from 14 to 36 μm, with DV/AP ratios lower than 2. Considering its mean size, this dinoflagellate is the smallest among the species of the genus *Ostreopsis*. Observing the cells with Scanning Electron Microscopy (SEM) the thecal surface results smooth and also covered with spaced pores. *O.* cf. *ovata* complete plate pattern, which is crucial in distinguishing the species from other dinoflagellate, is « Po, 3' , 7'', 6C, 6S, 5''', 2'''', 1p » as reported in Faust & Gulledge (2002) (Fig. 2).

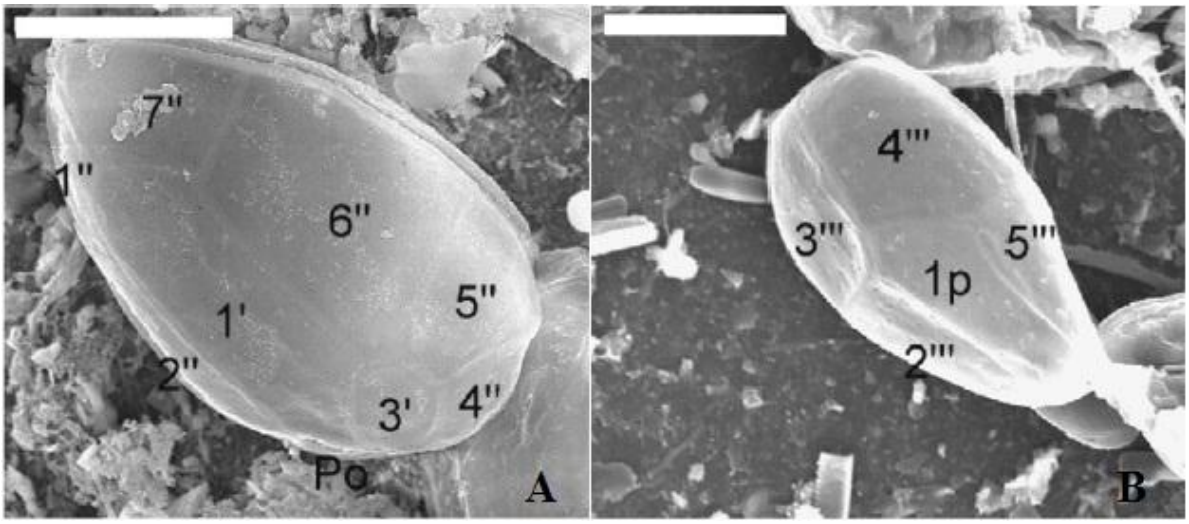

Figure 2. *O.* cf. *ovata* observed with the SEM (Aligizaki & Nikolaidis, 2006). Epithecal (A) and hipothecal (B) view and relative plates. White scale bar of 20 μm.

Regarding its **ecology**, *O. ovata* is a mixotrophic benthic dinoflagellate, auxotrophic for some vitamins, able to phagocytize its preys (bacteria, ciliates, other microalgae) using an expandable ventral pore (Faust, 1998). As suggested by Nikolaidis & Aligizaki (2006), *O.* cf. *ovata* could be

able to enter in a resting stage, forming a sort of cysts, as demonstrated by the presence of some red hyaline bodies in many large field cells (that are candidates to turn into cysts, in contrast to small cells that are typically found during blooms, or prosperous periods), and by the fact that some cysts have been already observed in the related species *O.* cf. *siamensis* (Pearce et al., 2001) and *C. monotis* (Faust, 1992). In senescent cultures of *O.* cf. *ovata* some small spherical cells surrounded by a gelatinous envelope, that could be identified as cysts (Simoni et al., 2004), have been observed, but further and more specific studies would be needed to shed light on this aspect in *O.* cf. *ovata* life cycle.

This alga prefers to reside in shallow and calm waters, as it apparently requires high levels of light and warm waters (Totti et al., 2010), living as epiphyte of other sessile organisms or free on many kinds of hard substrata (Pistocchi et al., 2011).

In tropical areas, this dinoflagellate is particularly present in coral reef lagoon environments (Faust et al., 1996) as component of the epiphytic/benthic microflora on corals/sand, often in association with other *Ostreopsis* spp., and *Gambierdiscus, Prorocentrum, Amphidinium* species, with which has been implicated in causing the syndrome of ciguatera in humans (Morton et al., 1992).

In the Mediterranean Sea (but also in other temperate areas, like southern Australia, New Zealand, and Japan), *O.* cf. *ovata* is frequent as epiphyte on seagrasses and red-brown macrophytes that live in sheltered coves, especially along rocky shores. *O.* cf. *ovata* blooms typically occur during warm periods, with high temperature and salinity, and low hydrodynamism (Pistocchi et al., 2011). During the development of the bloom, by taking advantage of calm waters, *O.* cf. *ovata* covers all benthic substrates forming a mucilaginous film, which is composed by a fibrillar part made of cells' trichocysts and a mucilage part (Honsell et al., 2013). Cells are easily re-suspended in the water column if the hydrodynamism increases (Mangialajo et al., 2008; Totti et al., 2010; Mangialajo et al., 2011) in fact the hydrodynamism seems to have an important role in the development and decline of blooms (Aligizaki & Nikolaidis, 2006; Mangialajo et al., 2008).

1.1.2 Toxins produced by O. ovata

Palytoxin (PLTX) is a potent non-protein marine toxin, initially isolated in 1971 from some *Palythoa* spp., soft corals of the Pacific Ocean (Moore & Scheuer, 1971; Uemura et al., 1981). Since 70s, PLTX and a number of palytoxin analogues have been extracted also from many other marine organisms, including *O. ovata* and other dinoflagellates of the same genus (Ciminiello et al., 2011[a,b]).

PLTX is a large and very complex molecule with chemical composition $C_{129}H_{233}N_3O_{54}$, formed by a long polyhydroxylated and partially unsaturated aliphatic backbone, containing 64 chiral centers (Ramos & Vasconcelos, 2010). High resolution liquid chromatography - mass spectrometry (HR LC-MS) studies disclosed the presence, both in field (from Mediterranean areas) and cultured *O.* cf. *ovata* cells, of putative PLTX and six new palytoxin analogues, named **ovatoxins** (OVTXs; Fig. 3). The ovatoxins discovered until now (Ciminiello et al., 2006, 2008, 2010, 2011[a,b], 2012[a,b]) are all similar to the palytoxin in structure and composition :

- OVTX-a, with chemical composition $C_{129}H_{223}N_3O_{52}$. It appears to be the most produced toxin by *O.* cf. *ovata*: OVTX-a alone accounts for more than 50% of the total toxin in cultured cells (Guerrini et al., 2010; Pezzolesi et al., 2012; Ciminiello et al., 2012[a]; this work)
- OVTX-b, with chem. comp. $C_{131}H_{227}N_3O_{53}$
- OVTX-c, with chem. comp. $C_{131}H_{227}N_3O_{54}$
- OVTX-d/-e, both with chem. comp. $C_{129}H_{223}N_3O_{53}$ but different structure
- OVTX-f, with chem. comp. $C_{131}H_{227}N_3O_{52}$. This last was discovered in 2012 in only one Adriatic *O.* cf. *ovata* strain, accounting alone for 50% of the total toxin content (Ciminiello et al., 2012[b]).

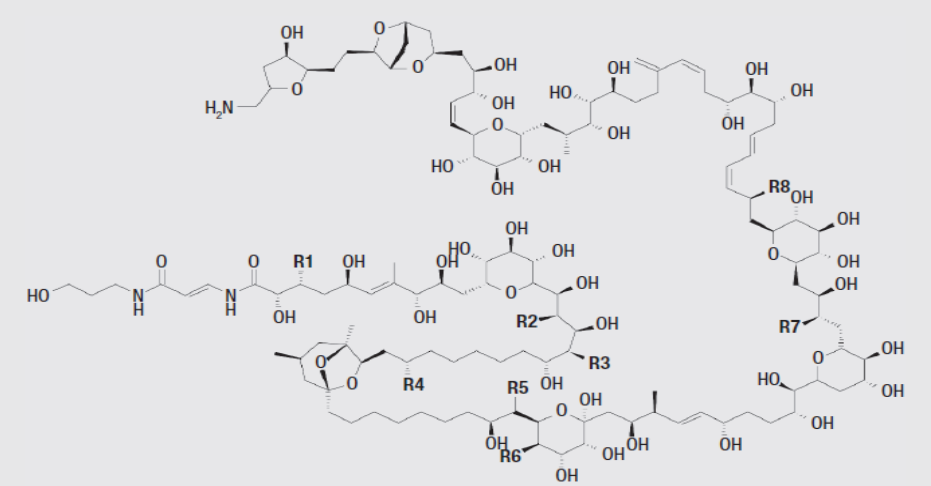

Toxin	R1	R2	R3	R4	R5	R6	R7	R8
PLTX	CH_3	OH	OH	CH_3	H	OH	OH	OH
OST-D	H	OH	H	H	OH	H	OH	OH
OVA-a	CH_3	H	OH	CH_3	OH	H	H	OH
42-OH-PLTX	CH_3	OH	OH	CH_3	OH	OH	OH	OH

Figure 3. Molecular structure of palytoxin (**PLTX**) and some palytoxin-like compounds, including ovatoxin-a (**OVA-a**) (Del Favero et al., 2012)

Palytoxin and its analogues may enter the food chain and accumulate mainly in filter-feeders molluscs, fishes and crustaceans, causing severe human intoxication and death due to the ingestion of contaminated products (Alcala et al., 1988; Onuma et al., 1999). Furthermore, toxic effects in individuals exposed via inhalation or skin contact to marine aerosol in coincidence with *Ostreopsis* spp. blooms, have been reported (see the following section 1.1.3).

At the cellular level, the Na^+/K^+–ATPase is the primary molecular target of PLTX: this compound binds the Na^+/K^+–ATPase and convert it into a non-selective ion channel (Habermann, 1989; Rossini & Bigiani, 2011), causing the membrane depolarization and consequent Ca^{2+} influx that may lead to multiple events regulated by Ca^{2+}-dependent pathways (Monroe & Tashjian, 1995). Depending on the cell type and toxin dose, also filamentous actin (F-actin) disassembly, cell rounding and swelling, cell death, and hemolytic activity have been described (Louzao et al., 2007; Prandi et al., 2011; Vidyarathna & Granéli, 2013). Furthermore, PLTX has been demonstrated to act as a skin tumor promoter, being able to modulate key signal transduction pathways involved in carcinogenesis (Fujiki et al., 1986; Wattenberg, 2007). Finally, administration of semi-purified toxic extracts from *O.* cf. *ovata* cultured cells (containing both PLTX and ovatoxins at known concentrations) in primary human macrophages induces a significant accumulation of gene transcripts the products of which are involved in inflammatory immune response (Crinelli et al., 2012), and demonstrates that palytoxin and, most likely, its congener *O.* cf. *ovata* toxins, have the potential to exert a pro-inflammatory activity.

1.1.3 O. cf. *ovata blooms in the Mediterranean Sea and dangers for public health*

HABs, or Harmful Algal Blooms, are blooms that cause harm, either due to the production of toxins by the blooming algae and/or to the manner in which the cells' physical structure, or accumulated biomass, affects co-occurring organisms and alters food web dynamics, so threaten the ecology of an area. Impacts of these phenomena could include mass mortalities of wild and farmed fish, shellfish and other invertebrates; human illness and death due to the ingestion of toxic seafood or to toxin exposure through inhalation or water contact; illness and death of marine mammals, seabirds, and other animals; alteration of marine habitats and trophic structure (Anderson et al., 2002).

From the 90s to today *O.* cf. *ovata* has been responsible for several HABs in the Mediterranean Sea: its toxins caused several issues to the other organisms who used to live in the blooming coastal areas and public health problems.

Human illness and death due to consumption of seafood contaminated with palytoxin and/or its analogues have been reported in tropical and subtropical zones, but not in the Mediterranean basin: here all the reported poisonings were due exclusively to exposure to seawater and/or aerosol containing palytoxins and analogues during *Ostreopsis* spp. blooms (Tubaro et al., 2011). In particular, since the end of the last decade, massive blooms of *Ostreopsis* spp. occurred along the Italian, French and Spanish coastlines during the warm season, sometimes resulting in respiratory and febrile syndrome outbreaks in humans exposed to sea-spray aerosol, which contains fragments of algal cells and/or PLTXs, and to seawater during recreational activities (see Table 1 in the next page).

The most serious incident occurred in the coasts of Genoa (Italy) between 17 and 26 July 2005, when a total of 209 subjects matched the above-described case definition. The clinical picture was mainly characterized by fever, irritative symptoms of the upper and lower respiratory tracts, conjunctives, headache, nausea and vomiting, variously associated. Mean onset of symptoms was about 4h after the beginning of exposure. In this episode forty-three subjects needed hospitalization (Durando et al., 2007).

From an ecological point of view, *O.* cf. *ovata* blooms in the Mediterranean have caused severe mass mortalities of benthic organisms (Di Turi et al., 2003; Sansoni et al., 2003; Simoni et al., 2003; Congestri et al., 2006; Shears and Ross, 2009). For example in Italy massive mortalities of marine invertebrates and macroalgae (Vale and Ares, 2007), and visible impacts on sessile (cirripeds, mussels, limpets) and mobile (echinoderms, cephalopods, little fishes) epibenthic organisms were observed after summer blooms of this dinoflagellate (Ciminiello et al., 2006; Totti et al., 2010). Despite this observed biological impact, little is known about the real consequences that these toxins may have on coastal communities: it should be considered that a damage to a single ecologically important species may rebound through the whole ecosystem, thus further investigations about toxic effects of PLTX and its analogues on different biological models (or single key-species) would be needed, as already done in some successful studies (Morton et al., 1982; Vale and Ares, 2007; Shears and Ross, 2009; Rhodes et al., 2000, 2002; Malagoli et al., 2008; Simoni et al., 2004; Faimali et al., 2011).

Location, year	Poisoning source	Cases (n°)	Route of Exposure	Symptoms and clinical data	Treatment	Outcome	PLTX detection: Methods[a]	Reference
Italy (Tyrrhenian Sea) 2005	*O. ovata*	209	Inhalational	Fever, sore throat, cough, dyspnoea, headache, nausea, rhinorrhea, lacrimation, vomiting, dermatitis. Mild leukocytosis, neutrophilia	Inhaled and systemic corticosteroids, NSAIDs, nebulized β-agonists, oxygen therapy to some hospitalized patients	Recovery (209/209) within 3 days	Putative PLTX: Mouse bioassay, LC-MS (Ciminiello et al., 2006)	Durando et al., 2007
Italy (Tyrrhenian Sea) 2006	*O. ovata*	19	Inhalational	Cough, sore throat, dyspnoea, fever, rhinorrhea, nausea, headache, lacrimation, vomiting	Inhaled and systemic corticosteroids, NSAIDs, nebulized β-agonists, oxygen therapy to some hospitalized patients	Recovery (19/19) within 3 days	Putative PLTX, ovatoxin-a: LC–MS (Ciminiello et al., 2008)	Durando et al., 2007

Location, year	Poisoning source	Cases (n°)	Route of Exposure	Symptoms and clinical data	Treatment	Outcome	PLTX detection: methods	Reference
Italy (Tyrrhenian Sea) 1998, 2000, 2001	*O. ovata*	~100	Inhalational	Conjunctivitis, upper airways irritation, myalgia, arthralgia, cough, fever	Not reported	Recovery (100/100) within 12 h after discontinuing exposure to seawater aerosol	Not reported	Sansoni et al., 2003
Italy (Southern Adriatic Sea) 2001	*O. ovata*	Not reported	Inhalational	Rhino-pharingitis, conjunctivitis, dermatitis	Not reported	Not reported	Not reported	Di Turi et al., 2003
Italy (Southern Adriatic Sea) 2003, 2004	*Ostreopsis* sp.	28	Inhalational	Rhinorrhea, cough, dyspnoea, fever, lacrimation, dermatitis	Paracetamol, inhaled/nebulized β2-agonist salbutamol	Recovery (28/28) within 24 h after discontinuing exposure to seawater aerosol	Not reported	Gallitelli et al., 2005; Gallitelli, personal communication
Spain (Sant Andreu de Llavaneres) 2004	*Ostreopsis* sp.	200	Inhalational	Rhinorrhea, rhinitis, throat irritation, cough, expectoration, eye irritation, headache	Not reported	Not reported	Not reported	Kermarec et al., 2008; Masó, personal communication
Spain (Almerian coast) 2006	*Ostreopsis* sp.	57	Inhalational	Sneezing, mucous hypersecretion, pharingitis/pharingeal pruritus, cough, rhinitis/nasal pruritus, rhinorrhea, fatigue, dry throat, eye irritation, dyspnoea, odynophagia, headache, arthralgia, weakness of the arms, lacrimation, fever, myalgia	Not reported	Recovery (57/57) within 1–13 days	Not reported	Barroso García et al., 2008
France (Frioul Islands) 2006	*O. ovata*	4	Inhalational, dermal	Lips and tongue irritation, headache, throat irritation, fever, diarrhoea	Not reported	Recovery (4/4) within 12–14 h without NSAIDs treatment	Not reported	Kermarec et al., 2008; Tichadou et al., 2010
France (Frioul Islands) 2008	*O. ovata*	21	Inhalational, dermal	Skin irritation, pruritus, mucosal irritation (eyes, nose, mouth)	NSAIDs	Recovery (21/21) within 6–12 h after NSAIDs therapy/12–48 h without treatment	Not reported	Tichadou et al., 2010
France (Nice) 2008	*O. ovata*	4	Inhalational, dermal	Skin irritaion, pruritus, mucosal irritation (nose, eyes, mouse)	NSAIDs	Recovery (4/4) within 10–12 h after NSAIDs therapy/16–24 h without treatment	Not reported	Tichadou et al., 2010
France (Villefranche) 2009	*O. ovata*	11	Inhalational, dermal	Skin irritaion, pruritus, mucosal irritation (eyes, nose, mouth)	NSAIDs	Recovery (11/11) within 4–6 h after NSAIDs therapy/14 h without treatment	Not reported	Tichadou et al., 2010
Monaco (Larvotto Beach) 2008	*O. ovata*	7	Inhalational, dermal	Skin irritation, pruritus, mucosal irritation (eyes, nose, mouth)	NSAIDs	Recovery (7/7) within 8 h after NSAIDs therapy/12–72 h without NSAIDs treatment	Not reported	Tichadou et al., 2010

NSAID = non steroidal anti-inflammatory drug.

Table 1. Blooms of *Ostreopsis* spp. which caused harm to human health in the Mediterranean (from Tubaro et al., 2011)

1.1.4 Bloom and toxin production dynamics of O. cf. *ovata*

There are many physical, chemical and biological factors that may affect an algal bloom.

Temperature is one of these factors, as it is important in defining the biogeographic boundaries within which a species can live (Dale et al. 2006). Therefore, different strains of the same species can be expected to have different optimal temperatures for growth: this may be attributed to genetic adaptations to local environmental conditions (Vidyarathna & Granéli, 2012). This adaptation may explain the observed differences in growth and toxicity of various strains of *O.* cf. *ovata* at different temperatures. In fact, a Japanese *O.* cf. *ovata* strain (Vidyarathna & Granéli, 2012) reported the greatest cellular growth and the highest toxicity at temperature of 24-25° C, while two other experiments on a Thyrrhenian strain (Granéli et al., 2011) and an Adriatic strain (Pezzolesi et al., 2012) revealed maximal toxicity at 20° C and 25° C, respectively, and maximal growth at 26-30° C and 20° C, respectively.

Salinity was also considered one of the most important key-factors in determining the blooming dynamics for this species but, as seen for temperature, field data are conflicting and depend on the considered area (i.e. strains). In addition, salinity alone seems not to explain *O.* cf. *ovata* proliferations: along Hawaiian coasts it was observed a negative correlation between salinity and *O.* cf. *ovata* presence (Parsons & Preskitt, 2007), while in the Mediterranean Sea this correlation results positive, since blooms occurred during warm periods which are characterized by higher salinity (37-39 PSU) than the annual averages (35 PSU) (Vila et al., 2001; Ungaro et al., 2005; Monti et al., 2007; Mangialajo et al. 2008; Pistocchi et al., 2010, 2011). An experiment conducted on an Adriatic *O.* cf. *ovata* strain by Pezzolesi et al. (2012), confirmed the natural trend observed in the Mediterranean areas: the greatest growth (although not so different from the others) was observed at the highest salinities of 36 and 40 PSU, while the highest toxicity at a lower salinity of 32 PSU.

Another factor, maybe the most important, in regulating algal bloom dynamics is the concentration of inorganic **nutrients**, primarily Nitrogen and Phosphorus. Also for this aspect field data are not clear, indeed *O.* cf. *ovata* blooms have occurred both in oligotrophic than in eutrophic waters (Vila et al., 2001; Shears & Ross, 2009; Accoroni et al., 2011). Some experiments have been conducted in order to investigate the role of nutrients in *O.* cf. *ovata* growth and toxicity, but the results were apparently conflicting. Using an Adriatic strain, Vanucci et al. (2012[b]) observed both the highest cellular growth and toxicity in balanced N:P conditions (molar N:P=16 in the culture medium), followed by P-deficiency (N:P=92) and N-deficiency (N:P=5) conditions. Vidyarathna & Granéli

(2013) instead, evidenced a significantly higher cells' toxicity of a Tyrrhenian strain in N-limited conditions (N:P=1,6). The differences between these results could be due to the both different experimental conditions and methods adopted in the two experiments and to the different physiologies of the two *O.* cf. *ovata* strains.

Due to the complex regulation of primary metabolic processes, it is not easy to predict the conditions which promote or depress the synthesis of toxins. In general, growth dynamics and toxicity of dinoflagellates reflect the physiological status of the organism; however little is presently known about the role that these compounds play in the biology of the algal cell.

An important factor in causing the end of an algal bloom, at least in a planktonic context, is the **grazing** pressure: for *O.* cf. *ovata*, which is a toxic benthic microalga, the role of grazing might decrease, since during its blooms mass mortalities of its potential predators, like sea-urchins and other benthic invertebrates, have been observed, due to the toxin production (Totti et al., 2010; and references therein).

Nevertheless it could be also possible that *O.* cf. *ovata* is influenced by substances produced by other organisms, in a positive or negative manner (**allelopathy**). For example, it is known that some of the species that are often associated to *O. ovata* (*Amphidinium sp*., *Coolia monotis*, *Gambierdiscus toxicus*, *Prorocentrum lima*) produce allelopathic substances that are able to inhibit the growth of other organisms (Granéli & Hansen, 2006), and potentially also the growth of *O. ovata*. Obviously, it is not to be excluded that *O. ovata* -itself may inhibit the growth of competitors via its toxins or other unknown compounds.

The relationships with **bacteria** should also play an important role in the growth and toxins' production dynamics of this dinoflagellate but, as well, very little is known about it. Vanucci et al. (2012[a]) cultured an Adriatic *O.* cf. *ovata* strain in axenic (without bacteria) and in ordinary culture conditions: the removal of bacteria unaffected algal growth except for conferring a more steady stationary phase. Furthermore in late stationary phase axenic cultures showed lower cell toxins' concentrations and higher extra-cellular toxins' values, but these differences were though not significantly.

These factors represent only a subset of those that could influence *O.* cf. *ovata* growth and toxicity. In this work we have shifted the focus on the internal cellular dynamics, trying to shed light on *O.* cf. *ovata* physiological mechanisms that govern its growth and toxin production, proposing and testing mechanistic hypotheses on specific processes (see the section 2. 'Aims of this study') through modelling in an *ad hoc* developed version of the European Regional Seas Ecosystem Model (ERSEM-2004, Blackford et al., 2004).

1.2 The 'European Regional Seas Ecosystem Model (ERSEM)'

1.2.1 An overview of ERSEM

The European Regional Seas Ecosystem Model (ERSEM, Baretta et al., 1995; Blackford et al., 2004) is a biomass and functional group -based biogeochemical model describing the nutrient and carbon cycle within the low trophic levels of the marine ecosystem. Model state variables include living organisms, dissolved nutrients, organic detritus, oxygen and CO_2 (Fig.4).

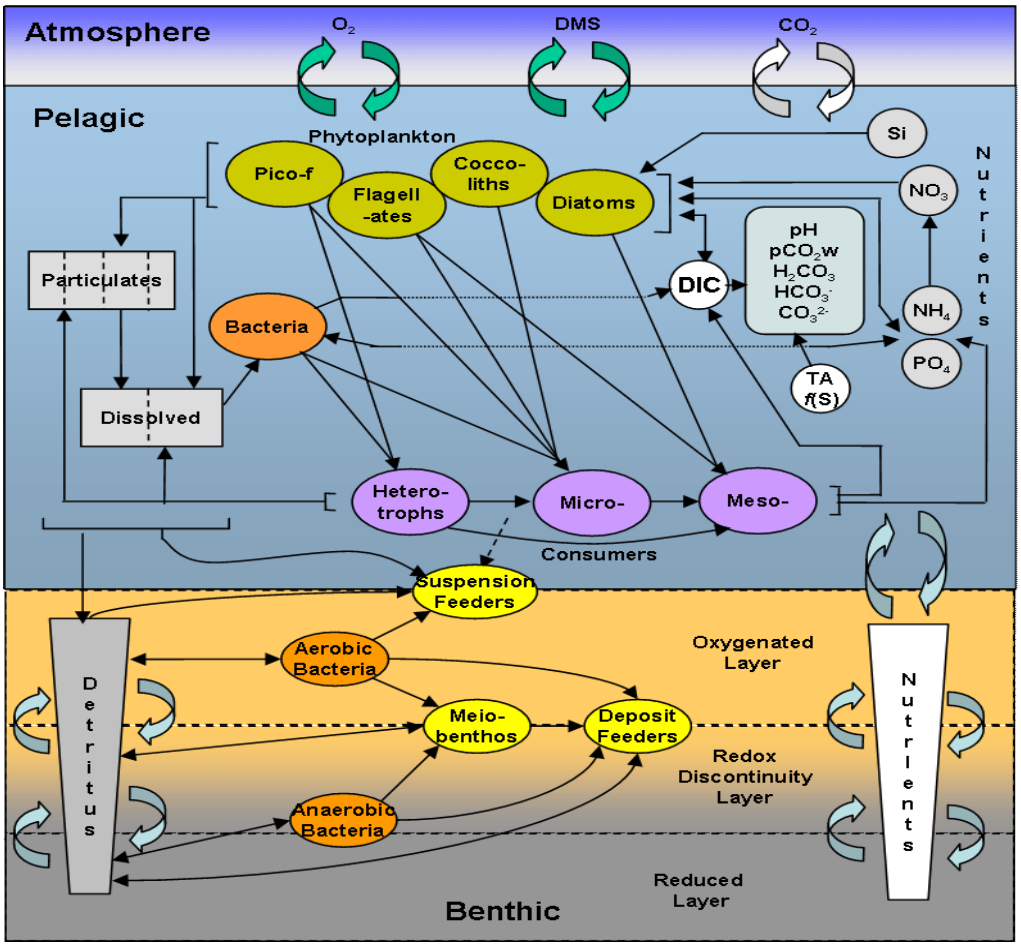

Figure 4. A schematic representation of ERSEM components. N.B. here coccoliths are assumed to be representative of nanophytoplankton

Pelagic living organisms are subdivided in three functional groups describing the planktonic trophic chain: primary producers, consumers and decomposers. Primary producers and consumers are subdivided into 4 and 3 size-based functional types, respectively, while decomposers are modeled through only one functional type. More specifically, the phytoplankton community

consists of picophytoplankton, nanoflagellates, dinoflagellates and diatoms. The zooplankton community is divided in mesozooplankton, microzooplankton and heterotrophic nanoflagellates, while decomposers are modeled by one type of heterotrophic bacteria. Functional types belonging to the same group share common process descriptions but different parameterizations.

A key feature of ERSEM is the decoupling between carbon and nutrient dynamics allowing the simulation of variable stoichiometry within the modeled organisms. Chlorophyll is also treated as an independent state variable following the formulation proposed by Geider et al. (1996). Consequently each plankton functional type is modeled throughout up to five state variables describing each cellular component: carbon, nitrogen, phosphorus, silicon, and chlorophyll-a.

Primary production is assumed to be not directly dependent on nutrient availability but active DOC (dissolved organic carbon) exudation is accounted in order to re-equilibrate the internal stoichiometry. This mechanism allows for a more accurate description of the nutrient limitation, also ensuring a large production of dissolved organic carbon (DOC) fuelling the bacterial pool.

Dissolved organic matter (DOM) is produced by different processes involving phytoplankton, bacteria and zooplankton while its consumption is exclusively regulated by bacteria uptake. DOM is subdivided in a labile and semi-labile component, in order to provide a representation of the range of organic compounds present in the marine DOM and their different degree of degradability. Particulate organic matter (POM) is assumed to be produced by phytoplankton and zooplankton and is divided into a number of size-based categories corresponding to different sedimentation rates. In this way it is possible to realistically simulate the dynamics leading to the carbon export from the surface to the deep ocean.

All together these features make ERSEM a flexible and adaptable model able to simulate, depending on the environmental nutrient concentration, the continuum of trophic pathways proposed by Legendre and Rassoulzadegan (1995), from the classical herbivorous food web (driven by large cell and high nutrient) to the so-called “microbial loop” (Azam et al., 1983) driven by bacteria feeding on DOC (Allen et al., 2002; Polimene et al., 2006, 2007). Thanks to this flexibility ERSEM has been successfully used to investigate different aspects of the marine biogeochemistry in a wide range of ecosystem contexts, from eutrophic coastal environments (Polimene et al., 2007, 2014) to continental shelf seas (Artioli et al., 2012, Blackford et al 2004) and oligotrophic regions (Polimene et al., 2012, Allen et al., 2002). In all the above cited studies, ERSEM has been coupled with a hydrodynamic model providing the physical framework (in terms of diffusive and advective fluxes) necessary to realistically reproduce the marine ecosystem. ERSEM, however, can also be used “standalone” to reproduce idealized systems (see for example

Polimene et al., 2006) or laboratory experiments (i.e. batch culture or chemostats) in which physical fluxes (advection and diffusion) can be considered negligible. ERSEM has recently been extended to include the carbonate system giving it a predictive capability for future acidification states (Blackford & Gilbert, 2007; Artioli et al., 2013).

ERSEM is also composed of a benthic module which dynamically simulates nutrient distribution within sediments, organic matter regeneration, bioturbation and bioirrigation along with the dynamics of 7 functional types broadly representing the living compartment of marine sediments. The latter includes suspension feeders (which feed directly from the pelagic system), deposit feeder (which feed on benthic detritus), infaunal predators, epifaunal predators and both aerobic and anaerobic bacteria (Blackford 1997).

1.2.2 Development of ERSEM and a few technical features

Since its first appearance (Baretta et al., 1995) ERSEM was continuously developed. In the pioneering work of Baretta and colleagues (Baretta et al., 1995) the model was used to simulate the ecosystem dynamics of the North Sea. To this purpose, ERSEM was implemented in a set of three dimensional boxes roughly representing the whole North Sea domain. Hydrodynamic fluxes (in the form of daily advective fluxes and diffusion coefficient), temperature and irradiance, were prescribed by an off-line coupling with a General Circulation Model. These physical constrains, along with the depth of each box provided all information specific to the North Sea, whereas the biological/chemical sub-models were constructed not to be site-specific.

Following works (e.g. Baretta-Bekker et al., 1997) improved the physical set-up of the North Sea implementation by rising the number of boxes (up to 130) in which the domain was discretized. Most importantly the decoupling of the carbon assimilation from the nutrient uptake was introduced in the model along with the nutrient uptake dynamics in the bacteria compartment. The improved version of the model was more flexible being able to simulate the full range of food webs, from a system dominated by the microbial loop in the relatively oligotrophic offshore areas to a system dominated by the omnivorous food web in the eutrophic continental coastal area.

More recently, ERSEM was further developed by including chlorophyll, as prognostic state variable, and the variable chlorophyll to carbon ratio (Blackford et al., 2004). With all these improvements ERSEM was able to reproduce the main ecosystem dynamics in six highly contrasting sites, with minimal changes in model parameters. Comparison of seasonally depth resolved and integrated properties illustrated that the model produced a wide range of community

dynamics and structures that can be plausibly related to variations in mixing, temperature, irradiance and nutrient supply. The model was proposed as a potential basis for an ecosystem-based management tool that may, with appropriate physical representation, be applied over large geographic and temporal scales with utility to both heuristic and predictive studies of the marine lower trophic levels. Latest ERSEM developments include iron dynamics, a more detailed description of bacterial metabolism (Polimene et al., 2006) and the production and fate of climatically active biogases (Polimene et al., 2012).

ERSEM represents the ecosystem as a group of parallel ordinary differential equations (ODEs), solved as an open ended recursive system using continuous simulation techniques (Blackford & Radford, 1995). The essence of the approach is first to define a group of variables which together represent the state of the whole system: its strength is that the rates of all the individual processes over any small time interval may then be defined simply as functions of the state of the system at that time, expressed by the instantaneous values of the state variables modified by external forcing. This enables the large number of individual processes to be conveniently subdivided into groups which may form independent modules linked only by the state variable matrix. This feature of the method facilitates the modular approach that has been adopted for ERSEM.

The choice of state variables was governed by a desire to keep the model as simple as possible without omitting any component which would exert a large influence on the balance of energy flow. The material composition of the state variables and of the transfers which interlink them might be any convenient tracer (e.g. energy). The standard units ensuring compatibility with most measured data sets were used: carbon state variables were represented in mg C m^{-3} in the pelagic and in benthic pore water region of the model and as mg C m^{-2} in the benthic layer; similarly nutrients and gases were expressed in mmol m^{-3} in the pelagic and in benthic pore water but as mmol m^{-2} in the benthic layer.

The mathematical algorithms used to solve the differential equations were initially included in the software SESAME (Software Environment for the Simulation and Analysis of Marine Ecosystems), written in the programming language Fortran-77 and running on Unix (Ruardij et al, 1995), then in the end of 90s they were directly integrated in ERSEM and re-written by the language “Fortran-90”.

A detailed description of ERSEM-2004, the model version used in this work, is provided in Blackford et al. (2004).

2. AIMS OF THIS STUDY

The mechanisms underpinning growth and toxin production in *O.* cf. *ovata*, and in dinoflagellates in general, are still far to be fully understood. Often the effects of external environmental factors on *O.* cf. *ovata* seem to be different and to depend on the strain: this observed variability in response to external factors could be due to genetic intra-specific variability, or even be due to different methods of detection (and data interpretation) by scientists, but also be caused by different combinations of factors, some of which are unknown. For this reasons, in this work we have decided to operate in an alternative way, focusing on *O.* cf. *ovata* single cellular processes in a mechanistic optic.

The principal aim of this thesis was to **expand the existing dataset for this species** through a new laboratory experiment and to **test, by means of numerical simulations, the following hypotheses** derived from the analysis of experimental results from several sources:

- toxin production consists of a basal (constant) component and an additional term triggered by nutrient stress. The basal component is proportional to the primary production, while the nutrient dependent term is proportional to carbon biomass
- concomitantly with the enhanced production of toxins, *O.* cf. *ovata* strongly reduces chlorophyll synthesis when stressed by nutrient
- *O.* cf. *ovata* is able to reduce its metabolism (forming a sort of resting stage) under extreme nutrient limiting condition; the accumulation of cellular carbon and toxins with respect to nutrient and chlorophyll is part of this strategy.

To this end, a newly developed formulation describing toxin compounds production and fate has been implemented in a simplified version of the European Regional Seas Ecosystem Model and used to simulate the experimental dynamics.

An additional goal of the presented work is to **improve the range of applicability** of a state of the art marine biogeochemical model (ERSEM) by implementing in it an ecological relevant process such as the production of toxic compounds. Finally, with our combined experimental and modelling approach we also meant to **highlight current knowledge gaps** on the physiology of *O.* cf. *ovata* and **provide recommendations** for future experimental works.

3. MATERIALS AND METHODS

In this work we have used the results of two experiments, named Alpha and Beta.
More specifically, **Alpha** is composed by the union of the two overlapping dataset derived from two experiments previously carried out on an Adriatic *O*. cf. *ovata* strain, reported in Pezzolesi et al. (in press) and Pezzolesi et al. (in prep.), since they were identical replicates (also in the obtained results), differing each other only in some conducted analyses. Instead **Beta** represents the new experiment conducted on the same strain that was arranged for this study: it represents a part of this thesis work, and its data are still unpublished (Pezzolesi et al., in prep.).

3.1 The experiment Beta

3.1.1 Experimental plan

This experiment was conducted on the same *O.* cf. *ovata* Adriatic strain OOAB0801 previously used in the experiment Alpha in order to obtain comparable data. This strain has been isolated during a bloom of *O.* cf. *ovata* near Bari (Puglia region, Italy) in summer 2008: some single cells of *O.* cf. *ovata* were selected from the multi-species field samples using the capillary pipette method (Hoshaw & Rosowski, 1973) and then grown in clonal cultures.
The "Alpha" experiment was conducted using a culture medium derived from an "f/2", a rich culture medium which is frequently used for the cultivation of marine microalgae (Guillard & Ryther, 1962; Guillard, 1975). In particular a modified "f(N10/P10)" medium was adopted, i.e. an f/2 with concentrations of nitrogen and phosphorus 5-times decreased, with the addition of selenium and without silicon.
In the experiment Beta we decided to grow *O.* cf. *ovata* in a limiting condition in terms of nutrients, adopting a "**modified f(N150/P150)**" medium, i.e. an f/2 with 75-fold decreased nitrogen and phosphorus concentrations, and the same concentration of all the other components, even in this case enriched with selenium and lacking silicon.
This particular medium was prepared using seawater provided by the "Centro Ricerche Marine" (Cesenatico, Emilia Romagna region, Italy) and aged in the dark for a few months in the laboratory. About 10L of seawater with salinity of 35 PSU (measured by a refractometer) were

filtered on GF-F glass-microfiber filters (Whatman, porosity 0.7 μm) and then re-filtered on Millipore filters (porosity 0.22 μm) in order to remove bacteria, and were finally sterilized by autoclaving at 120° C for 20 minutes.

All the components of the f/2 medium (less silicon and adding selenium) with a 75-fold decreased quantity of N and P, were appropriately added to the sterile seawater using stock solutions and obtaining a modified f(N150/P150). Chemical compositions of f/2, modified f(N10/P10), and modified f(N150P150) mediums are reported in the Table 2.

MEDIUM COMPONENTS	*standard f/2*	**Alpha experiment**	**Beta experiment**
		f(N10-P10), + Se, - Si	*f(N150-P150), + Se,- Si*
$NaNO_3$	8,82E-04	1,76E-04	1,18E-05
NaH_2PO_4 H_2O	3,62E-05	7,24E-06	4,83E-07
Na_2SiO_3 $9H_2O$	1,06E-04	-	-
$FeCl_3$ $6H_2O$	1,17E-05	1,17E-05	1,17E-05
Na_2EDTA $2H_2O$	1,17E-05	1,17E-05	1,17E-05
$CuSO_4$ $5H_2O$	3,93E-08	3,93E-08	3,93E-08
Na_2MoO_4 $2H_2O$	2,60E-08	2,60E-08	2,60E-08
$ZnSO_4$ $7H_2O$	7,65E-08	7,65E-08	7,65E-08
$CoCl_2$ $6H_2O$	4,20E-08	4,20E-08	4,20E-08
$MnCl_2$ $4H_2O$	9,10E-07	9,10E-07	9,10E-07
GP (for Se)	-	1,00E-08	1,00E-08
thiamine HCl (vit. B_1)	2,96E-07	2,96E-07	2,96E-07
biotin (vit. H)	2,05E-09	2,05E-09	2,05E-09
cyanocobalamin (vit. B_{12})	3,69E-10	3,69E-10	3,69E-10

Table 2. Chemical composition of different culture mediums: the nutrients are written in red, and the concentrations are expressed in **mol/L**. Concentrations varying from standard f/2 are highlighted in blue.

The batch cultures were arranged in three sterile 3 L Erlenmeyer flasks, each prepared mixing a medium volume of about 2250 mL and an inoculum of 450 mL containing *O.* cf. *ovata* cells obtained from a stock culture (previously acclimated to the new conditions of the experiment for about a week), in order to have a total volume of 2700 mL per flask and a concentration of about 150 cells/mL.

These three identical cultures, named A - B - C, represented the replicates of the Beta experiment, and were grown at the same temperature of 20 ± 1° C in a thermostatic room, under a common PAR (Photosynthetically Active Radiation) of about 125 μE $m^{-2}s^{-1}$, or 27 W m^{-2}.

Throughout the course of the experiment several culture aliquots were taken from each replicate in order to perform the various analyses, as reported in Table 3.

DAY	0	1	2	6	7	9	13	15	21	27	35
O. cf *ovata* cells' counts and biovolumes	10	10	10	10	10	50	50	50	50	50	50
Chlorophyll-a analysis		20	20	20	20	20	20	20	20	20	20
Pulse Amplitude Modulation analysis (n. r. in this work)		5	5	5	5	5	5	5	5	5	5
Polysaccharides' analysis			15	15		15	15		15		15
Intracellular P and dissolved nutrients (N - P)	50	100	100	100		100	50	50	50	50	50
Elemental analysis by CHN		50	50	50	50	50	50	50	50	50	50
Toxins' analysis			100	100		100	100		100		100
Bacterial cells' counts and biovolumes	12		12	12		12	12	12	12	12	12
Total withdrawals	72	185	312	312	85	352	302	187	302	187	302
Residual volume in each culture (originally 2700 mL)	2628	2443	2131	1819	1734	1382	1080	893	591	404	102

Table 3. Samples aliquots taken from each replicate flask with relative target analysis

3.1.2 Cell counts and biovolumes

CELL COUNTS

Culture volumes (10 mL) for counting and cell volume's estimations were fixed with a few drops of LUGOL, a solution containing iodine and iodide.

To control the cellular growth in cultures several counts have been performed at different days (see Tab. 3): 1 ml of each sample was placed in the counting chamber and then *O.* cf. *ovata* cells were counted using an inverted optical microscope Axiovert 100 (Zeiss) at 320 x magnification following the method of Uthermöl (1931). According to this method cells can be counted in each of "a" visual fields of area "b", randomly selected within the total area of the chamber "c", and finally it is possible to calculate the average number of cells per milliliter by the following formula:

$$\text{cells / mL} = \frac{\sum \text{cells}}{a} \cdot \frac{c}{b}$$

Alternatively, it is possible to count the cells in each "d" visual field-swiping (with area "e") taken along the maximum diameter of the chamber, randomly selected by turning the chamber of area "c", and to calculate the cells' abundance per mL by the alternative formula:

$$\text{cells / mL} = \frac{\sum \text{cells}}{d} \cdot \frac{c}{e}$$

At the end of the experiment growth curves of each culture were obtained over time, and expressed as cells/mL. Then, considering cells' counts from the exponential phase (day 1-6), the specific growth rate (μ, expressed as day^{-1}) was calculated using the following equation:

$$\mu = \frac{\ln N_1 - \ln N_0}{t_1 - t_0}$$

where N_1 and N_0 were cell densities values at time t_1 (day 6) and t_0 (day 1).

CELL VOLUMES

Dimensions of *O.* cf. *ovata* cells [dorsoventral diameter (DV), Width (W), anteroposterior diameter (AP)] were measured through the software Nis Elements BR 2.20 from the real-time pictures that were taken from the cells using a Digital Sight DSU1 camera (Nikon) connected to the same microscope previously used for the counts (Fig. 5).

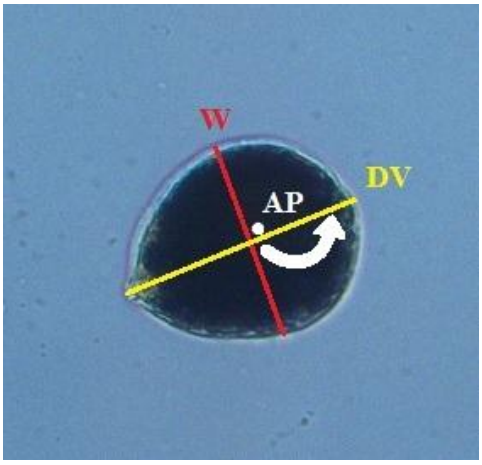

Figure 5. A cell of *O.* cf. *ovata* from the experimental cultures; the 3 dimensions are reported.

Minimum 20 measurements for each dimension were taken for each sample. The daily mean cell volumes for each culture have been calculated through the following formula:

$$\text{Daily Mean Cell Volume} = \frac{\sum \frac{\pi}{6} \cdot \text{DV} \cdot \text{W} \cdot \overline{\text{AP}}}{\text{n}}$$

where DV = dorsoventral diameter, W = width, $\overline{\text{AP}}$ = daily mean anteroposterior diameter, n = number of cells per day with known DV and W (from each culture).
This formula calculates the volume of the cells with the assumption of an ellipsoid shape, according to Sun & Liu (2003).

3.1.3 Chlorophyll-a

Chlorophyll-a was measured with a spectrophotometric method.
A volume (10 mL) of sample from each culture (Table 3) was centrifuged at 5000 rpm for 15 minutes at 4° C. Once removed the supernatant, the resulting pellet was re-suspended in 3 mL of 90% acetone, then agitated with a vortex mixer, and stored in the dark for 24 hours in order to allow chlorophyll extraction. After the incubation samples were centrifuged at 3000 rpm for 10 minutes: the supernatant was collected and absorbance was measured at the wavelengths of 750 and 665 nm. The chlorophyll-a was determined according to the following equation (Ritchie, 2006):

$$\text{Chlorophyll a } (\mu\text{g} \cdot \text{L}^{-1}) = \frac{[\text{A}(665\text{s}) - \text{A}(750\text{s})] \cdot \text{v} \cdot 10^3 \cdot 11.4062}{\text{co} \cdot \text{V}}$$

where:

- A(665s) = the blank corrected absorbance at 665 nm
- A(750s) = the blank corrected absorbance at 750 nm
- v = volume of acetone solution used for the extraction (mL)
- co = cell path length (cm)
- V = volume of filtered sample (mL)

3.1.4 Analysis of dissolved inorganic nutrients and organic phosphorus

A volume (50-150 mL) of sample from each culture (Table 3) was filtered on glass-microfiber GF-F filters (Whatman, porosity of 0.7 μm). Both the filtrates (for the inorganic nutrients measurements) and the filters (for the analysis of intra-cellular phosphorus) were kept frozen at -20° C until further analysis, according to traditional spectrophotometric methods (Strickland & Parsons, 1968).

DISSOLVED INORGANIC NITROGEN

Three different solutions were prepared to perform the analysis:

- "sample" solution: specific volumes (38.5-100 mL) of each filtered culture sample were brought to a final volume of 100 mL by adding synthetic seawater
- "blank" solution, composed exclusively by 100 mL of synthetic seawater
- "standard" solution, prepared with 0.1 mL of standard solution (N-NO_3 140 mg/L) and 99.9 mL of synthetic seawater.

In each of the three different solutions 2 mL of concentrated 25% ammonium chloride (m/V) were added.

Then these solutions (sample, blank, standard) were passed for gravity through glass columns filled with granules of metallic coppery cadmium (previously washed with 200 mL of diluted 0.625% ammonium chloride (m/V) and 200 mL of distilled water) in order to reduce any nitrates to nitrites. To avoid collecting any mixed percolate, the first 45 mL of each solution percolated were discarded, while the further 50 mL of each were collected in glass cylinders. In each sample 2 mL of sulfanil-amide 1% (m/V) were added, and after 3 minutes, also 1 mL of 0.1% naphthyl-ethylene-diamine (m/V). After 15 minutes, sample absorbance was measured with the spectrophotometer at 543 nm.

The F factor of each column, which is an index of its efficiency, was calculated:

$$F = \frac{[N - NO_3]}{A(543)st - A(543)b}$$

where $[N - NO_3]$ represents the concentration of N-NO_3 in the standard solution (0.14 mg/L), A(543)st is the absorbance of the standard at 543 nm and A(543)b is the absorbance of the blank at the same wavelength.

F should have a value between 0.31 (corresponding to 100% of efficiency) and 0.37 (84% of efficiency): higher values indicate that the column need to be re-activated.
Finally it was possible to calculate the nitrates concentrations (expressed as mg/L) in each sample by the formula:

$$[\mathrm{N-NO_3}] = \frac{\mathrm{F} \cdot 100 \cdot [\mathrm{A(543)s - A(543)b}]}{\mathrm{V}}$$

where A(543)s represents the absorbance of the sample and V is the original volume of the sample, expressed in mL.

DISSOLVED INORGANIC PHOSPHORUS

The method involves the formation of a phospho-molybdic complex whose concentration is measured colorimetrically at the wavelength of 885 nm.
First a reactive mixture was prepared by mixing four different solutions in a ratio of 2 : 5 : 2 : 1, respectively, i.e. a solution of ammonium molybdate (0.03 g/mL in distilled water), a solution of sulfuric acid (140 mL of 96% acid in 1 L of distilled water), a solution of ascorbic acid (0.054 g/mL in distilled water) and a potassium-antimonile tartrate solution (1.36 mg/mL in distilled water). 50 mL of distilled water for each "blank" solution and 50 mL of each filtered culture sample were placed into graduated 50 mL cylinders. In each cylinder 5 mL of the reactive mixture solution were added, then they were capped and shaken, and finally allowed to stand for 10 minutes, so that the reaction occurs. The resulted compound has a blue color, the intensity of which is proportional to the concentration of phosphates in the starting solution.
Absorbance of the samples were measured at 885 nm using a spectrophotometer, and phosphate concentrations were calculated basing on a calibration curve previously obtained by analyzing several standard solutions of phosphates (KH_2PO_4), in a range between 0 and 0.456 μg/mL.

ORGANIC PHOSPHORUS

Cells that had been retained on the calcined GF-F filters were digested with 8 mL of a 5% solution of potassium per-sulfate ($K_2S_2O_8$), as proposed by Menzel & Corwin (1965), and phosphates released from the organic matter were quantified using the same method as inorganic phosphorus, already mentioned in the previous paragraph.

3.1.5 Polysaccharides

To quantify the total polysaccharides produced by *O.* cf. *ovata* in our cultures the colorimetric method proposed by Dubois et al. (1956) was followed: it is based on the fact that carbohydrates in the presence of concentrated acids form cyclic compounds called furfurals, which condense with phenols giving colored products that can be analyzed by spectrophotometry.

First it was necessary to extract carbohydrates from the cells, and for this aim we used the method of Myklestad & Haug (1972). A volume (15 mL) of each culture (Table 3) was added to 2 volumes (30 mL) of absolute ethanol in centrifuge tubes, placed at -20° C for 24 hours, and then centrifuged at 12000 rpm for 15 minutes at a temperature of 4° C. Once centrifuged, the supernatant was removed, and 1 mL of 80% sulfuric acid was added to each pellet: the samples thus treated were left to rest at 20° C for 20 hours and then were diluted with 5 mL of distilled water.

After the extraction, polysaccharides were determined by the Phenol Sulfuric Method (Dubois et al., 1956) using glucose as standard (range 0 - 62.5 μg/mL): 2 mL of each sample were mixed to 50 μL of 80% phenol and 5 mL of concentrated sulfuric acid, and were left to rest for 30 minutes at room temperature. Absorbance of the samples was then measured at a wavelength of 543 nm and total polysaccharides' concentrations were calculated based on the glucose calibration curve.

3.1.6 Elemental analysis (CHN)

Elemental analysis of cellular carbon and nitrogen was performed by using the elemental analyzer Flash 2000, series CHNS/O (Thermo Scientific).

This instrument burns the organic samples, which are contained in tin capsules, in a combustion chamber at 950° C. The pumping of oxygen raises the temperature up to 1800° C and allows a complete combustion of organic matter, resulting in gasification of each element contained in it. The resulting gases, after some reductions, are channeled into a narrow column for gas chromatography, and are finally quantitatively detected through a detector based on the thermal conductivity of some elements: carbon, hydrogen, nitrogen and oxygen.

The 50 mL culture samples (Table 3) were divided in 5 replicates of 10 mL, each of which was filtered through GF-F calcined filters on a small surface area of about 0.3 cm^2, then filters were stored at -20° C. Before the analysis they were dried in an oven at 50° C for 10 minutes, then were cut to remove part of the unused filter, and each small filter was placed in a tin capsule.

All capsules were directly analyzed, since the presence of the fiber-glass filter in the combustion chamber does not affect the results of the analysis.
A calibration curve obtained using a standard compound, 2,5-Bis (5-tert-butyl-2-benzo-oxazol-2-yl) thiophene (BBOT), was used for quantification of total C and N on each filter. Finally cellular amount were calculated considering culture cell concentration.

3.1.7 Toxins

Toxins were extracted in the laboratory and then analyzed at the Department of Pharmacy, Università Federico II of Naples (Italy), by high resolution liquid chromatography coupled with mass spectrometry (HRLC-MS) (Ciminiello et al., 2011[b]).
Samples of 100 mL were collected from each replicate on several days (Table 3), and then filtered with GF-F filters. Filters containing the cells were frozen at -80° C, till further treatments in order to extract intra-cellular toxins, while the filtrates containing the extra-cellular toxins were kept frozen at -20° C, until shipment to Naples.
The filters were chopped and placed in centrifuge tubes. Thus a volume (1-1.5 mL, depending on the cells' concentration at that day) of 50% methanol was added in each tube, then subjected to sonication on ice for 3 minutes (by a Sonicator mod. XL), and finally centrifuged at 12000 rpm for 15 minutes at 4° C (Beckman centrifuge, mod. J2-HS). The resulting supernatant, which contains the toxins extracted from the lysed cells, was collected from each tube: this cycle of extraction and collection was repeated other 2 times, in order to maximize the extraction of toxins from the samples.
Finally the total supernatant of each sample was brought to a final volume of 5 mL by adding 50% methanol, sealed and stored at 4° C until being shipped to Naples.

3.1.8 Cell counts and biovolumes of bacteria

Bacteria abundances in the algal cultures were assessed by direct bacteria counts using epifluorescence microscopy after staining with SYBR gold (Shibata et al., 2006).
More in details, subsample (10 mL) were collected from the algal batch cultures at days 0, 2, 6, 7, 9, 13, 15, 21, 27, and 35. Samples were immediately preserved using 0.2 μm pre-filtered formaldehyde (2% final sample concentration), stored in the dark at 4° C until processed within few days. Subsamples (1000 μL or 100 μL, depending on growth day) were concentrated onto 0.2

µm pore size filters (Anodisc 25 mm, Al_2O_3) and stained with 100 µL BYBR gold (stock solution diluted 1:1250). The 100 µL subsamples, before being concentrated onto filters were diluted 1:10 with Milli-Q prefiltered sterile water. Filters were incubated in the dark for 15 min and mounted on glass slides with a drop of 50% phosphate buffer saline and 50% glycerol, containing 0.5% ascorbic acid.

Duplicate slides were prepared for each sample. Slides were either counted immediately after preparation or stored at - 20° C for 2-3 days before being counted. Bacterial counts were carried out by epifluorescence microscopy using a Zeiss Axioplan microscope (BP 450-490/FT510/LP520) equipped with an HBO 100 mercury lamp. A minimum of 20-30 randomly chosen fields were viewed at 1000 x magnification.

For each sample a minimum of 20-30 cells were measured for cell volume calculation. Bacteria cells were measured at 1000 x using an image capture system (Nis Elements BR 2.20 software) consisted of a Nikon Digital Sight DSU1 camera connected to the microscope. Cell volume was calculated by assigning simplified geometrical shapes to cells.

3.2 Preparations required for the modelling

3.2.1 Experiments "Alpha" & "Beta" and converting Units of Measure

As already mentioned, the modelling work was based on data, and related interpretations, from the experiments Alpha (Pezzolesi et al., in press; Pezzolesi et al., in prep.) and Beta (this work), since these experiments are almost totally comparable one with the other, and perhaps they are between the most detailed ones ever conducted on *O.* cf. *ovata*. These two experiments were conducted using the same Adriatic strain of *O.* cf. *ovata* (named OOAB0801), growing it in a medium with the same nitrogen to phosphorus ratio of about 24.4 (thus in phosphorus-limitation), but with a total concentration of nutrients that in the exp. Beta was 15-times lower than in the exp. Alpha. The variables analyzed in the experiment Alpha were exactly the same that have been studied the Beta experiment (except lipids and proteins, not detected in the latter), and also the techniques of analysis were the same.

In order to compare modelled and observed variables, experimental values were converted in model units as displayed in Table 4.

VARIABLE	MODEL UNIT
Algal carbon	mg C / m^3
Bacterial carbon	mg C / m^3
Chlorophyll-a	mg Chl / m^3
Chl-a / C organic algal ratio	mg Chl / mg C
Algal phosphorus	mmol P / m^3
P / C organic algal ratio	mmol P / mg
Algal nitrogen	mmol N / m^3
N / C organic algal ratio	mmol N / mg C
Inorganic phosphorus	mmol P / m^3
Inorganic nitrogen	mmol N / m^3
Cellular toxins (tox)	mg C / m^3
tox / C organic algal ratio	-
Extra-cellular toxins	mg C / m^3

Table 4. ERSEM variables used in this study and relative units. State (prognostic) variables in white fields and secondary (diagnostic) variables in gray fields.

However for diagnostic purposes modelling results reported hereafter are given in mg/L, which is the unit more frequently used in literature in this kind of biological studies.

3.2.2 Data processing

ALGAL CARBON

The first problem we had to face was how to consider the total organic carbon (POC) detected by the CHN analyzer in both the experiments.

The detected POC, in fact, was very high to be considered as only the cellular carbon content of *O.* cf. *ovata*. The C:N:P ratios calculated in the last part of the cultures of both the experiments reached values (601:24:1 in the last day of the exp. Alpha, see Table 7 in section 4.2.1) which are well higher than the classical Redfield ratio (106:16:1), that is usually considered the "optimal" internal stoichiometry for marine microalgae (Redfield, 1934, 1958; Tett & Droop, 1988; Hillebrand & Sommer, 1999). Remarkable variations from the Redfield ratio were observed in both field (Geider & La Roche, 2002; Ho et al., 2003) and laboratory (Goldman 1986; John & Flynn, 2000; Klausmeier et al., 2004) studies on marine microalgae, especially when exposed to nutrient limiting conditions. Even considering this, however, the POC:PON:POP ratios detected in our experiments, resulted outside the range of carbon to nutrient ratios described in literature for marine microalgae. Furthermore, also the Chl-a to POC weight ratio reached values (lower limit of 0.0028 and 0.0004 in the exp. Alpha and Beta, respectively) not compatible to the Chl-a:C values observed in cultured marine microalgae usually ranging from 0.1 to 0.01 (Geider 1987, 1993).

Finally, such growth of particulate carbon in the last days (21-27-35) of the experiment Alpha, was not justified neither by an increase in cells number, nor by an increase in mean cell volume, and we could say the same for the last part (decaying phase, days 22-35) of the experiment Beta, although to a lesser extent. For all these reasons, we hypothesized that the POC detected by the CHN analyzer in the samples from the last phases of the experiments was biased by the presence of extra-cellular polysaccharidic mucilages, which are usually copiously produced by *O*. cf. *Ovata* during the stationary phase (Guerrini et al., 1998; Liu & Buskey, 2000; Pezzolesi et al., in press). This organic matrix is not easily removable with the analytical procedures that we have used (e.g. filtration, see section 3.2.1.) and is likely to have been preserved in the samples when they were analyzed.

The growth curves of *O*. cf. *ovata* cellular carbon were, therefore, estimated by correcting the original POC curve in the last phases of the cultures. As already stated, the production of extra-cellular polysaccharides is associated with the stationary phase of the culture. This was also confirmed by the fact that we found a really strong correlation ($r > 0.98$) between the POC and the total cell volume (obtained by multiplying the number of cells of each day for the mean cell volume of the same day) in the first 15 days of culture of both the experiments (Fig. 23), when the presence of mucilages was still quite low. So the measured POC was a good estimator of algal carbon in the first phase (from exponential to mid stationary) of the cultures. According to this finding, in the second part of the cultures (from day 21 to day 35) the cellular carbon was estimated starting from the total cell volume (measured at each day) and using the linear regressions of the aforementioned correlation between total cell volumes and carbon (see Fig. 22 in section 4.2.3). We used the same regression also to estimate the amount of cellular carbon for the initial day of the cultures (day 0) since direct measurement by CHN were missing.

In summary, the curves of cellular carbon that have been used as experimental guides (and tests) for the model were composed of both the values from CHN measurements and values from the aforementioned data processing (see Fig. 23 in section 4.2.3).

TOXINS

All the different kinds of toxins detected in the experiments (putative palitoxin, ovatoxin-a, -b, -c, -d, -e) were grouped in a single toxic compound. This choice was driven by the fact that all the toxic compounds produced in the cultures were very similar in term of both molecular structure and stoichiometry (129-131 atoms of C, 223-227 atoms of H, 3 atoms of N, 52-54 atoms of O).

Furthermore, the relative proportion of each toxic compound resulted to be stable throughout the experiments, as previously observed by Ciminiello et al. (2011[b]).

Considering the stoichiometric composition of each toxic species and assuming stable proportions between them, both taken from the study of Ciminiello et al. (2011[b]), we constructed out an "ideal" (average) toxin, with elemental formula $C_{129.66}$ $H_{224.32}$ N_3 $O_{52.53}$: total toxins of experiments Alpha and Beta were treated as quantities of this "ideal" toxin. Furthermore, in the modelling part of this study only the carbon fraction of this "ideal" toxin was considered as experimental value, since toxins were modelled as a single state variable composed of only carbon.

BACTERIAL CARBON, NITROGEN AND PHOSPHORUS

We estimated the biomass of bacteria starting from bacterial cells' counts and mean cell volumes. At first was calculated the total volume of bacterial cells from each replicate by multiplying the number of cells for the measured mean volume of a cell (0.433 μm^3), and then it was multiplied for a mean value of a carbon content per volume of 145 fg C μm^{-3}, approximated from the works of Fagerbakke et al. (1996) and Steenbergh et al. (2013) on the advice of Prof. Silvana Vanucci: in this way we obtained a rough estimate (with wide margins of error) of the bacterial carbon's trends in the cultures. Moreover we estimated the bacterial nitrogen and phosphorus, that were calculated starting from carbon through the C:N:P molar ratio of 45:9:1 from Goldman et al. (1987).

3.3 Modelling

3.3.1 General setting of ERSEM and initial conditions

The model used in this work was a simplified version of the pelagic-module of the European Regional Seas Ecosystem Model (ERSEM-2004; Blackford et al., 2004), provided by the Plymouth Marine Laboratory (PML; Plymouth, United Kingdom).

The first part of the modelling work was to enable ERSEM to reproduce a mono-specific batch culture. To this end the model was i) highly simplified, ii) initialized with the data observed (or estimated) at day "0" of the experiments and iii) run under the experimental light and temperature conditions. More specifically:

- ERSEM was run alone with no physical coupling

- we considered only one of the four phytoplankton types described in the original model and the bacteria functional type: more specifically, we used the functional group of dinoflagellates and the functional group of heterotrophic pelagic bacteria (P4 and B1 in Blackford et al., 2004, respectively)
- the model was initialized with nutrient, chlorophyll and biomass concentrations observed (or estimated) at the beginning of each experiment (Table 5)
- the model was run under a 16 - 8 hours light-dark cycle and a constant Photosynthetically Active Radiation (PAR) of 24.35 W m^{-2} (about 112 μE m^{-2} s^{-1}) and 27.18 W m^{-2} (about 125 μE $m^{-2}s^{-1}$), in order to exactly reproduce the experimental light environment.

Light extinction in ERSEM is assumed to be dependent only on particles (which are able to absorb and/or scatter the incident radiation). However, in peculiar environments such as a batch culture where dissolved organic matter concentrations can reach extremely high value (as in some eutrophic coastal areas and estuaries) the contribution of the dissolved organic compounds to the extinction of light can be of primary importance. For this reason, and given the high concentration of dissolved polysaccharides observed in the cultures, we have also considered the model state variable "semi-labile DOC" (identifiable with mucilaginous matrices) in the equation describing the attenuation of light in the model (see equation "2" in Blackford et al., 2004).
This step required the creation of the new parameter σ_{sl} (reported in Table 6, section 3.3.4): a light-absorption coefficient for the semi-labile organic matter with a value that is one tenth of the value of the same coefficient for POM.

INITIAL CONDITIONS IN ERSEM			
VARIABLE	**UNIT**	**EXP. ALPHA value**	**EXP. BETA value**
Inorganic N	mmol / m^3	176.4	16
Inorganic P	mmol / m^3	7.24	0.69
Algal C	mg / m^3	1847	1798
Algal N	mmol / m^3	13.56	13.014
Algal P	mmol / m^3	1.54	0.49
Chlorophyll	mg / m^3	14.8	3
Bacterial C	mg / m^3	16.7	28.9
Bacterial N	mmol / m^3	0.278	0.48
Bacterial P	mmol / m^3	0.031	0.053
Cellular toxins	mg / m^3	0.7	0.7
External toxins	mg / m^3	0	0

Table 5. Some of the initial conditions that were introduced in ERSEM in order to reproduce the exp. Alpha and Beta trends and test our hypothesis. Here are reported only the variables whose values have been changed from the original ones.

3.3.2 Modelling toxins production and excretion

Experimental data (see section 4.2.2) of the experiment Alpha showed us that there were significant linear correlations between toxins cellular content (given as toxin to carbon ratio) and both phosphorus to carbon and nitrogen to carbon intra-cellular ratios (r = - 0.85 and r = - 0.79 respectively). Instead for the experiment Beta this correlation was not clear as in the previous case, but only because the P:C and N:C ratios of the alga were very low since the beginning of the experiment, rapidly reaching (and maintaining) values that were on the edge of the lower limit, thereby preventing the display of a linear correlation. On the light of this result, we hypothesized that **the toxin production is stimulated by increasing stress conditions of the alga**, intending as "stress" the decline in intracellular nutrients to carbon ratios.

O. cf. *ovata* toxic compounds were modelled through two distinct state variables: **tox**, indicating cellular toxins, and **toxe**, indicating extra-cellular toxins, both composed of only carbon, since toxin nitrogen content was considered to be negligible with respect to the total cellular nitrogen budget. Cellular toxin production was assumed to be composed by two additive terms, the first accounting for a constant production assumed to take place under any conditions (in blue field) and the second assumed to be stimulated by intra-cellular nutrient deficiency, or nutrient-stress (in red field):

$$\left.\frac{\partial\,\mathbf{tox}}{\partial\,\mathrm{t}}\right|^{INC} = (\mathrm{GPP} - \mathrm{A.RESP}) \cdot \mathrm{Q_{Tmin}} + (1 - \mathrm{NS}) \cdot \left(1 - \frac{\mathrm{Q_T}}{\mathrm{Q_{Tmax}}}\right) \cdot \mathrm{C} \cdot \varphi$$

Where GPP is the gross primary production, A.RESP is the activity respiration, $\mathrm{Q_{Tmin}}$, $\mathrm{Q_T}$ and $\mathrm{Q_{Tmax}}$ are the minimum, actual and maximum toxin to carbon cellular ratio, respectively, and C is the actual algal biomass (carbon). φ is the fraction of cellular carbon daily invested in the production of **tox** during nutrient-stress conditions. NS is the function describing nutrient limitation and is given by:

$$\mathrm{NS} = \mathrm{MIN}(\mathrm{NS_P}, \mathrm{NS_N})$$

NS_P and NS_N are determined as:

$$NS_P = \mathrm{MIN}\left\{1\,,\mathrm{MAX}\left[0\,,\frac{Q_P - Q_{Pmin}}{(s_P \cdot Q_{PRed}) - Q_{Pmin}}\right]\right\}$$

$$NS_N = \mathrm{MIN}\left\{1\,,\mathrm{MAX}\left[0\,,\frac{Q_N - Q_{Nmin}}{(s_N \cdot Q_{NRed}) - Q_{Nmin}}\right]\right\}$$

where Q_P/Q_N and Q_{Pmin}/Q_{Nmin} are the actual and minimum phosphorus/nitrogen to carbon cellular ratio, respectively. s_P/s_N are threshold-parameters that determine at what proportion of Redfield ratio (i.e. Q_{PRed}/Q_{NRed}) the cell starts to be nutrient-stressed.

Figure 6 shows with a graphical example how the NS_P value changes in function of phosphorus-stress condition of the alga, with a hint about its influence on the nutrient-stress driven exudation (Blackford et al., 2004).

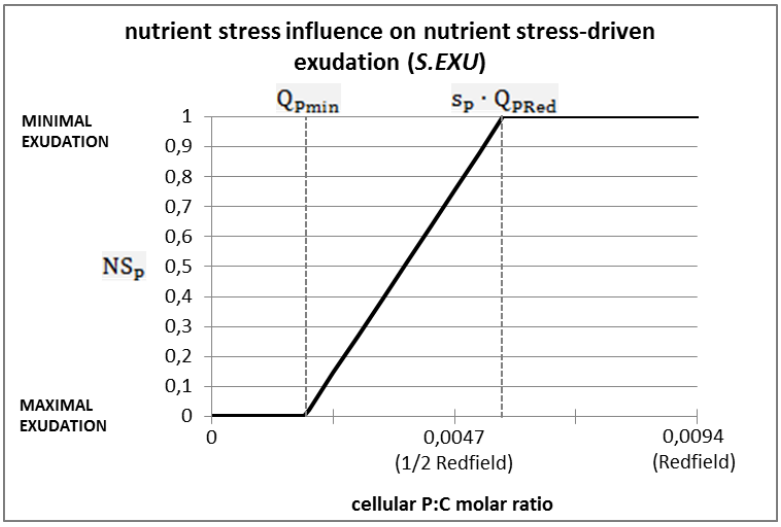

Figure 6. Value trend of the adimensional factor $\mathbf{NS_P}$ as a function of the intra-cellular P:C molar ratio.

Toxin loss terms were assumed to be composed by lysis, basal respiration and nutrient stress-driven exudation:

$$\left.\frac{\partial\,\mathbf{tox}}{\partial\,t}\right|^{LOSS} = (r_C^{LYS} + r_C^{R.RESP} + r_C^{S.EXU}) \cdot \mathbf{tox}$$

Where r_C^{LYS}, $r_C^{R.RESP}$, $r_C^{S.EXU}$ are rates of cellular lysis, rest respiration and nutrient stress-driven exudation, respectively (Blackford et al., 2004), and **tox** is the actual toxins' amount in the cells.

The amount of toxins released outside the cell (a part form the carbon respired) is channeled into "**toxe**":

$$\frac{\partial\,\mathbf{toxe}}{\partial\,\mathrm{t}} = (\mathrm{r}_C^{LYS} + \mathrm{r}_C^{S.EXU}) \cdot \mathbf{tox}$$

We also assumed that the toxins present in the medium (**toxe**) were not degradable by bacteria at the temporal scale relevant for this study.

3.3.3 Chlorophyll, rest respiration and mortality

Our experimental data revealed that *O.* cf. *ovata* is able to grow also in a situation of strong internal nutrient-stress (very high C:N and C:P ratios), also reaching very low chlorophyll to carbon cellular ratios and, nevertheless, continuing to maintain a positive net primary production, even capable of supporting an associated bacterial community.
Starting from these results, we propose two physiological processes as mechanistic explanations of the observed trends: a tight dependency of the chlorophyll to carbon ratio from the internal stoichiometry (C:P and C:N), and the capacity to reduce the loss due to rest respiration and mortality in response to severe nutrient limitation. Model formulation has been modified in order to account for these mechanisms.

CHLOROPHYLL

The chlorophyll cellular quota in phytoplankton is known to be dependent on different environmental factors such as temperature, light and nutrient (Geider et al., 1997). However, in the standard version of ERSEM, chlorophyll to carbon ratio is assumed to vary depending on light only. While this assumption has been demonstrated to be reasonable in simulating the marine ecosystem where light is generally inversely related to nutrients, it is clearly not enough to reproduce the chlorophyll to carbon evolution in a batch experiment where light is roughly constant and nutrient availability highly variable (depending on the phase of the culture).
In the light of some clear experimental results (see sections 4.1.2 and 4.2.1) we proposed for the nutrient-stress a major role in limiting the synthesis of chlorophyll. Thus we modified the chlorophyll dynamics described in Blackford et al. (2004) by making the chlorophyll production directly (through interventions on the model source code) and severely (through an appropriate

parameterization) dependent on nutrient stress. Thus we introduced in the source equation of chlorophyll synthesis a new adimensional multiplying factor $\mathbf{NS}^{\boldsymbol{chl}}$ (Nutrient Stress for Chlorophyll) with a value between 0 and 1, depending by the severity of nutrient-stress:

$$\left.\frac{\partial\,\mathrm{chl}}{\partial\,\mathrm{t}}\right|^{INC} = (\mathrm{GPP} - \mathrm{A.RESP}) \cdot \rho \cdot \mathbf{NS}^{\boldsymbol{chl}}$$

Where GPP is the gross primary production, A.RESP is the "activity respiration" and ρ is the fraction of primary production invested in chlorophyll synthesis (Geider et al., 1997).
$\mathbf{NS}^{\boldsymbol{chl}}$ is given by:

$$\mathbf{NS}^{\boldsymbol{chl}} = \mathrm{MIN}\left(\mathrm{NS}_{\mathrm{P}}^{chl}, \mathrm{NS}_{\mathrm{N}}^{chl}\right)$$

$\mathrm{NS}_{\mathrm{P}}^{chl}$ and $\mathrm{NS}_{\mathrm{N}}^{chl}$ are determined as:

$$\mathrm{NS}_{\mathrm{N,P}}^{chl} = \mathrm{MIN}\left\{1, \mathrm{MAX}\left[0, \frac{\mathrm{Q_{N,P}} - \mathrm{Q}_{\mathrm{N,Pmin}}^{chl}}{\left(\mathrm{s}_{\mathrm{N,P}}^{chl} \cdot \mathrm{Q_{N,PRed}}\right) - \mathrm{Q}_{\mathrm{N,Pmin}}^{chl}}\right]\right\}$$

where $\mathrm{Q_{N,P}}$ is the actual nutrient (N or P), $\mathrm{Q}_{\mathrm{N,Pmin}}^{chl}$and $\mathrm{Q_{N,PRed}}$ are the minimal and Redfield nutrient (P or N) to carbon cellular ratio, respectively. $\mathrm{s}_{\mathrm{N,P}}^{chl}$ is a multiplying factor that determines at what proportion of Redfield P:C ratio nutrient-stress limitation in chlorophyll synthesis starts.
Figure 7 is a graphical example of the change of $\mathrm{NS}_{\mathrm{P}}^{chl}$ value in function of phosphorus-stress condition of the alga.

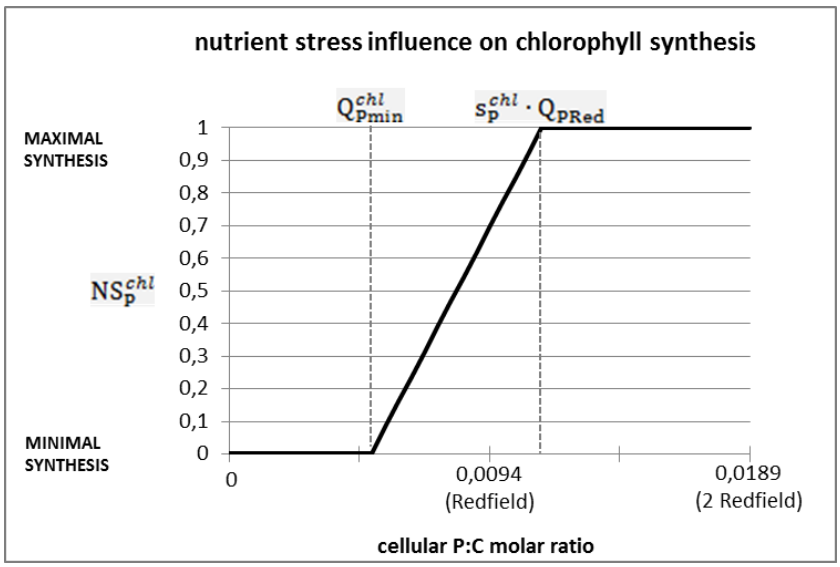

Figure 7. Value trend of the adimensional factor $\mathbf{NS}_{\mathbf{P}}^{\boldsymbol{chl}}$ as a function of the intra-cellular P:C molar ratio.

REST RESPIRATION AND MORTALITY

In order to reproduce the high biomass concentration observed in the last part of the two experiments, we also re-formulated the model equation describing the rest respiration (R.RESP) and the mortality due by lysis (LYS). More specifically, we assumed a **reduction of activity respiration under extreme nutrient limiting conditions** and a **lysis rate not dependent on nutrient limitation** (as in Blackford et al., 2004) but fixed. The reduction of rest respiration under severs environmental conditions (e.g. extreme nutrient limitation) in dinoflagellates is commonly associated to the formation of resting stages (Pfiester & Anderson, 1987). The choice of making the lysis rate not dependent on nutrient stress was driven by the very reduced number of dead cells observed in the cultures of both the experiments, suggesting that the alga was not subject to lysis possibly due to an efficient acclimation to the growing conditions.

The equation for the rest respiration was re-written as:

$$R.RESP = f^{T} \cdot \mathrm{r_{R.res}} \cdot \mathbf{NS}^{\boldsymbol{res}}$$

Where f^{T} is the function describing the metabolic dependency from temperature and $\mathrm{r_{R.res}}$ is the daily rest respiration rate. $\mathbf{NS}^{\boldsymbol{res}}$ is given by:

$$\mathbf{NS}^{\boldsymbol{res}} = \mathrm{MIN}\{1\ ;\ \mathrm{MAX}[0.1\ ;\ \mathrm{MIN}(\mathrm{NS_P^{res}}\ ;\ \mathrm{NS_N^{res}})]\}$$

NS_P^{res} and NS_N^{res} are determined as:

$$NS_{N,P}^{res} = \frac{Q_{N,P} - Q_{N,Pmin}}{\left(s_{N,P}^{res} \cdot Q_{N,PRed}\right) - Q_{N,Pmin}}$$

Where $Q_{N,P}$ is the actual nutrient (N or P), $Q_{N,Pmin}$ and $Q_{N,PRed}$ are the minimal and Redfield nutrient (P or N) to carbon cellular ratio, respectively. $s_{N,P}^{res}$ is a multiplying factor that determines at what proportion of Redfield P:C ratio nutrient-stress limitation of rest respiration starts.
Finally, the equation describing lysis rate was reduced to:

$$r_C^{LYS} = r_{lys} \cdot \frac{\cancel{1}}{(\cancel{NS + 0,1})}$$

3.3.4 Parameter setting

The last part of the model set-up was to calibrate the model by tuning the original parameters to obtain better data fitting. In Table 6 are shown parameters which have been changed with respect to Blackford et al. (2004) and the parameters relative to the newly formulated equations.

Table 6. Model parameters changed, or added (in gray field), in respect to Blackford et al. (2004)

Parameter description	Notation	ERSEM unit	Proposed value	Reference
OPTICAL AND PHOTOSYNTHESIS–IRRADIANCE CURVE PARAMETERS				
Extinction coefficient of semi-labile organic matter	σ_{sl}	m^2 (mg C)$^{-1}$	0.1 e-4	This work
Background extinction	σ_{bg}	m^{-1}	0.06	PML value
Maximum chlorophyll to carbon cell ratio	θ_{max}	mg Chl (mg C)$^{-1}$	0.02	Experimentally observed
Initial slope of PI-curve	α	mg C m^2 (mg Chl W d)$^{-1}$	2.5	This work
Photo-inhibition parameter	β	mg C m^2 (mg Chl W d)$^{-1}$	0.04	PML value
PARAMETERS FOR BACTERIA FUNCTIONAL GROUP AND DETRITAL PROCESSES				
Respired fraction of uptake	r_{upk}^B	-	0.6	Polimene et al. (2006)
Basal respiration at 10°C	$r_{R,res}^B$	d^{-1}	0.05	Polimene et al. (2006)
Mortality rate	r_{lys}^B	d^{-1}	0.06	This work
Maximum N/C ratio	Q_{Nmax}^B	mmol N (mg C)$^{-1}$	0.017	Polimene et al. (2006)
Maximum P/C ratio	Q_{Pmax}^B	mmol P (mg C)$^{-1}$	0.0018	Polimene et al. (2006)
Fraction of medium size detritus available for bacteria	r_{detr}	-	0.1	This work

Spec. rate for breakdown of semi-labile DOM to dissolved organics	r_{dis}	d^{-1}	0.011	This work
PARAMETERS FOR THE DINOFLAGELLATES FUNCTIONAL GROUP				
Daily rate of basal (rest) respiration	$r_{R.res}$	d^{-1}	0.01	This work
Exudation under nutrient stress	$P_{S.exu}$	-	0.2	PML value
Minimum N/C ratio	Q_{Nmin}	mmol N (mg C)$^{-1}$	0.003	Experimentally observed
Maximum N/C ratio	Q_{Nmax}	mmol N (mg C)$^{-1}$	0.01197	Experimentally observed
Minimum P/C ratio	Q_{Pmin}	mmol P (mg C)$^{-1}$	1.5 e-4	Experimentally observed
Maximum P/C ratio	Q_{Pmax}	mmol P (mg C)$^{-1}$	9.432 e-4	Experimentally observed
Minimum N/C ratio for chlorophyll synthesis	Q_{Nmin}^{chl}	mmol N (mg C)$^{-1}$	0.00687	This work
Minimum P/C ratio for chlorophyll synthesis	Q_{Pmin}^{chl}	mmol P (mg C)$^{-1}$	4.288 e-4	This work
Affinity for NO_3^-	a_{N3}	m^3 (mg C)$^{-1}$ d^{-1}	0.01	PML value
Affinity for NH_4^+	a_{N4}	m^3 (mg C)$^{-1}$ d^{-1}	0.01	PML value
Affinity for PO_4^{3-}	a_P	m^3 (mg C)$^{-1}$ d^{-1}	0.01	PML value
N-stress threshold	s_N	-	0.6	This work
P-stress threshold	s_P	-	0.6	This work
N-stress threshold for chlorophyll synthesis	s_N^{chl}	-	0.95	This work
P-stress threshold for chlorophyll synthesis	s_P^{chl}	-	1.2	This work
N-stress threshold for respiration decrease	s_N^{res}	-	0.56	This work
P-stress threshold for respiration decrease	s_P^{res}	-	0.51	This work
Minimum daily lysis rate	r_{lys}	d^{-1}	0.005	This work
Minimum **tox**:C ratio, or carbon fraction invested in basal toxin production	Q_{Tmin}	-	0.001	This work
Maximum **tox**:C ratio at which nutrient-stress toxin production stops	Q_{Tmax}	-	0.003	This work
Carbon fraction to be invested in nutrient-stress toxins production	φ	d^{-1}	0.0025	This work

With this parameterization the model reproduced well the dynamics of exp. Alpha, while inserting the initial conditions of exp. Beta the simulations were not very satisfactory (see section 4.4.2).
Thus we have re-calibrated few parameters of nutrient stress-threshold trying to reproduce more faithfully the dynamics of the experiment Beta. s_N and s_P were both lowered from a value of 0.6 to 0.28. We have also lowered the value of the P-stress threshold for chlorophyll synthesis s_P^{chl} from 1.2 to 1.07 and the value of Q_{Pmax} from $9.43 \cdot 10^{-4}$ to $8.41 \cdot 10^{-4}$. Except s_N, these changes involved parameters accounting for P:C ratios only (not N:C ratios) for a practical reason, since

the limiting conditions (stress) were always triggered by phosphorus deficiency in all our simulations.

3.3.5 Used software and statistics

In order to display the immediate trends of each variable in the numerous simulations performed by the ERSEM model the free software Python 2.7, which runs on Linux, was used.
All the other processes carried out, including the graphs and some statistics in this thesis, were executed manually by the software Microsoft Excel 2010.
To test the goodness of the simulations compared to the experimental data, for each variable were made the following statistics:

- Pearson correlations
- P-values for the Pearson correlations
- Root Mean Square Errors (RMSEs)
- Mean Percentage Errors (MPEs).

The first three were calculated in Excel 2010, while for the P-values was used the version 3.0 beta of the Free Statistics Calculators (website: http://www.danielsoper.com/statcalc3/default.aspx).

4. RESULTS AND DISCUSSION

4.1 The experiment Beta

4.1.1 Growth curves and cell volumes

O. cf. *ovata* growth was similar in all the three culture-replicates, allowing us to obtain a reliable growth curve (Fig. 8). From the curve can be noted the exponential phase (days 0-6), the stationary phase (days 7-21), whose beginning is identifiable by the first inflection point of the curve, and also a possible beginning of decaying phase (days 22-35).

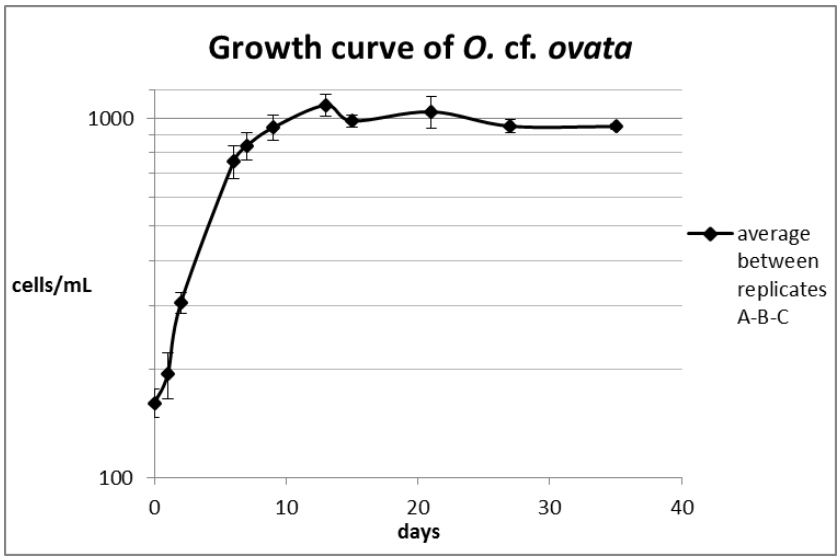

Figure 8. Mean cellular growth in the cultures, expressed as cells per mL.

If compared to the experiment Alpha, in which the cells had reached an average density of over 6000 cells/mL in the stationary phase (Pezzolesi et al., in press), cell growth was about 6 times lower, due to the much lower concentration of nutrients in the culture medium, in accordance with the previous findings of Vanucci et al. (2012[b]).

During the exponential phase (day 1-6) the specific grow rate (μ) was 0.27 d^{-1}, which is about half the one calculated in the experiment Alfa (day 1-7; μ = 0.52 d^{-1}; Pezzolesi et al., in press), due, also in this case, to the different concentrations of nutrients in the two experiments.

The trend of the mean cellular biovolumes during the exp. Beta is showed in the Figure 9. Despite the high variability observed among replicates, during the exponential phase a decrease of the average cell volume was observed, due to the active cell division, followed by a re-increase during the stationary phase (already noted by Guerrini et al., 2010; Pezzolesi et al., 2012; Accoroni et al., 2012). Finally a slow decline in the presumed decaying phase was observed, probably due to the aging of the cells (in fact in this phase many cases of depigmentation and deformations were observed).

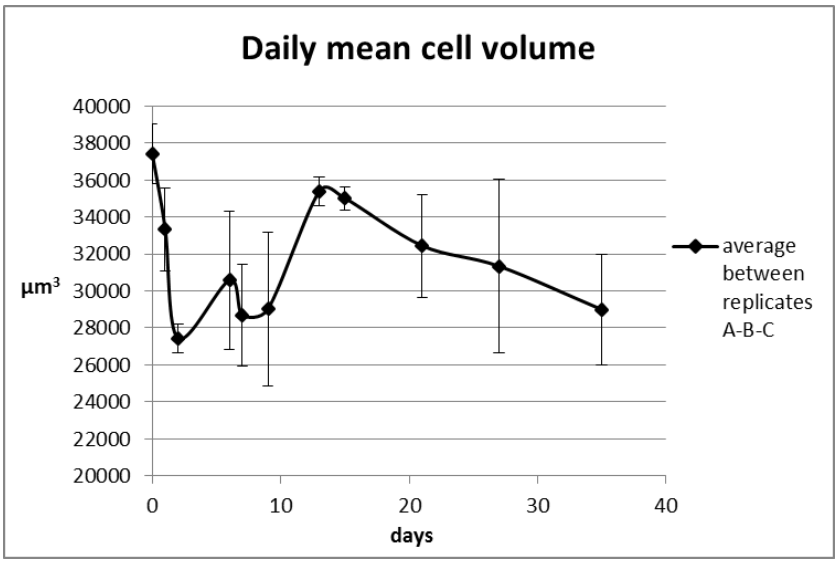

Figure 9. Daily average values of cell volume.

4.1.2 Chlorophyll-a

In this experiment the levels of measured chlorophyll-a were low, nonetheless sufficient to ensure the algal growth and the accumulation of biomass, at least until the decaying phase.
The chlorophyll-a concentration curve, which was also considered in the modelling part of this work, is showed in Figure 10. The highest detected value of chlorophyll-a was 15 μg/L (day 9).

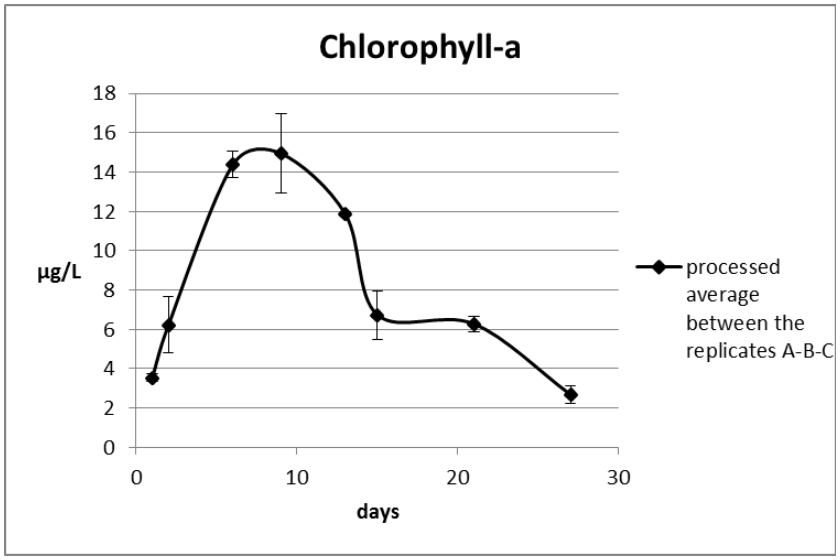

Figure 10. Average trend of chlorophyll-a levels during the experiment, expressed as mg/L.

The general trend is clear: chlorophyll-a levels increased during the exponential phase and started to decrease as soon as the cultures entered into the stationary phase, when the inorganic nutrients in the culture medium were depleted, as chlorophyll-a represents one of the most important N-rich compounds in the algal cells (Flynn et al., 1994). The chl-a profile was therefore clearly not representative of the algal biomass (e.g. cell density) during the growth. The shape of the chlorophyll curve for this experiment was similar to the one for the exp. Alpha, but the values were lower by an order of magnitude (Pezzolesi et al, in press.) due to the initial different nutrients concentration.

4.1.3 Inorganic nutrient

As for the experiment Alpha, phosphates and nitrates in the culture mediums were rapidly taken up by *O.* cf. *ovata* cells during the exponential phases of the cultures, and both were totally depleted between day 6 and 7 (Figure 11), then cells entered into the stationary phase.

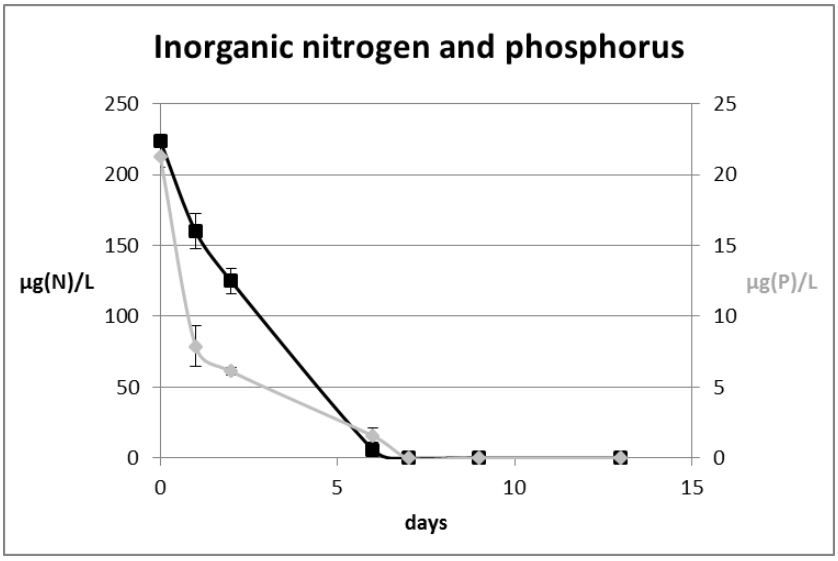

Figure 11. Concentrations of dissolved nutrients N and P (as µg/L) in the first days of culture.

In Figure 12 is showed the trend of the inorganic N:P ratio in the medium.

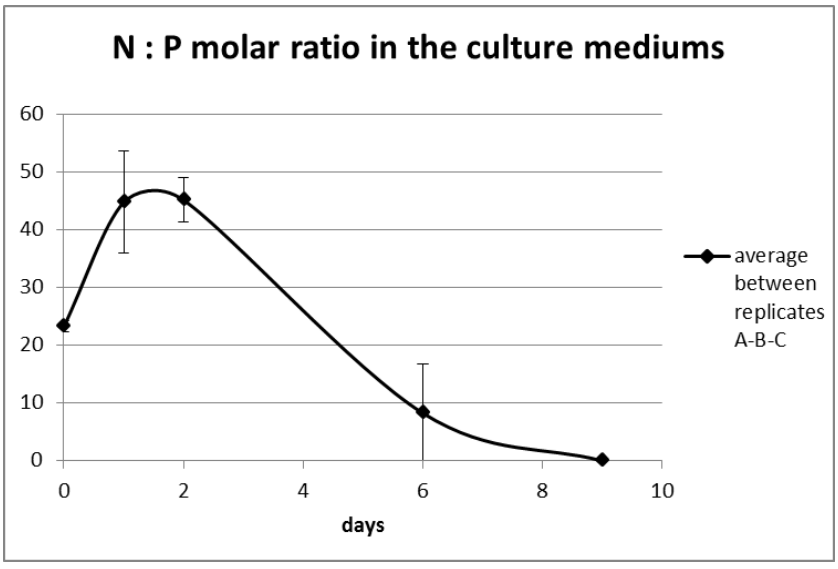

Figure 12. Ratio of dissolved nitrogen to phosphorus.

The increase in the N:P ratio in the culture medium during the first days of growth reflects a faster consumption of phosphate compared with nitrates, in accordance with the experiment Alpha (Pezzolesi et al., in press) and also with a previous study conducted on a different Adriatic strain (Vanucci et al., 2012[b]). This result was attended, since growth and carbon fixation may continue for several generations in P-depletion and be limited under high N:P ratio (John & Flynn, 2000). A rapid uptake within few days of growth was found also for other benthic dinoflagellates (e.g. *P. hoffmannianum, P. lima*), for which P was the major nutrient affecting the growth (Aikman et al., 1993; Vanucci et al., 2010).

4.1.4 Polysaccharides

The profile curve of total polysaccharides is shown in Figure 13.

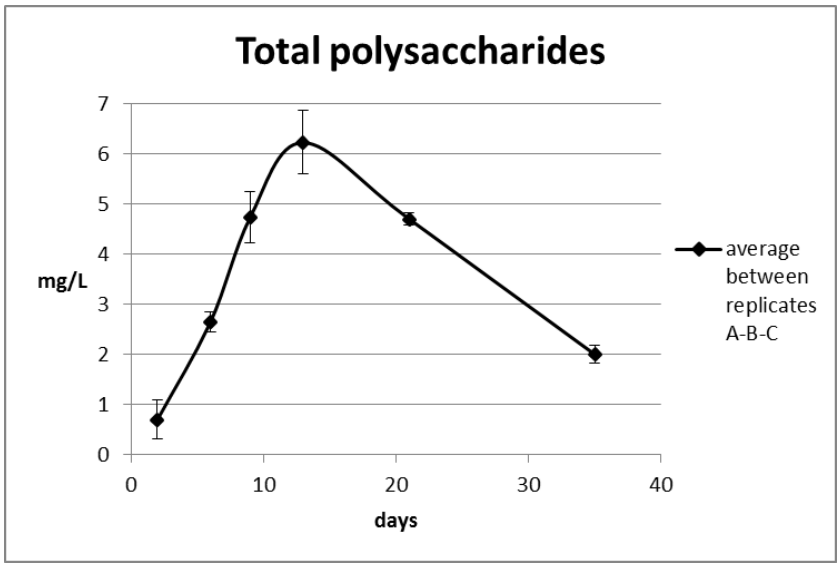

Figure 13. Daily mean concentration of total polysaccharides in the three cultures, expressed as mg/L.

The amount of total carbohydrates increased until the first part of the stationary phase with a maximal value of 6.23 mg/L at day 13, and decreased in its second part and throughout the decaying phase. Generally *O.* cf. *ovata* cells accumulate polysaccharides especially in the stationary phase, probably due to nutrient limitation (Liu & Buskey, 2000; Guerrini et al., 1998; exp. Alpha, Pezzolesi et al., in press): the fact that in this experiment we detected a decrease of the polysaccharides in the last phase of cultures (21-35), can be an indication of the entrance of the cells into a true decaying phase.

In our findings there is also a clear relationship between the presence of polysaccharides and the concentration of chlorophyll (see Fig. 10) which follows a similar trend. However this relationship was not observed in the exp. Alpha, where the accumulation of polysaccharides continued throughout the duration of the experiment contrarily to a general decrease of chlorophyll-a concentration in the stationary phase (Pezzolesi et al., in press).

In previous studies (Granéli et al. 2002; Honsell et al., 2013; Pezzolesi et al., in press) it was observed as the production, and also extrusion, of polysaccharides can be seen as a colonization strategy, as cells may more easily aggregate, and form a mucous mat that strongly attach to the substrate. Moreover, these extracellular compounds may protect the cells against grazing (Liu & Buskey, 2000), once more facilitating the development of algal community (Pezzolesi et al., in press).

4.1.5 Organic carbon, nitrogen and phosphorus in O. cf. *ovata cells*

The profiles of organic carbon and nitrogen-phosphorus are showed in Figures 14 and 15, respectively.

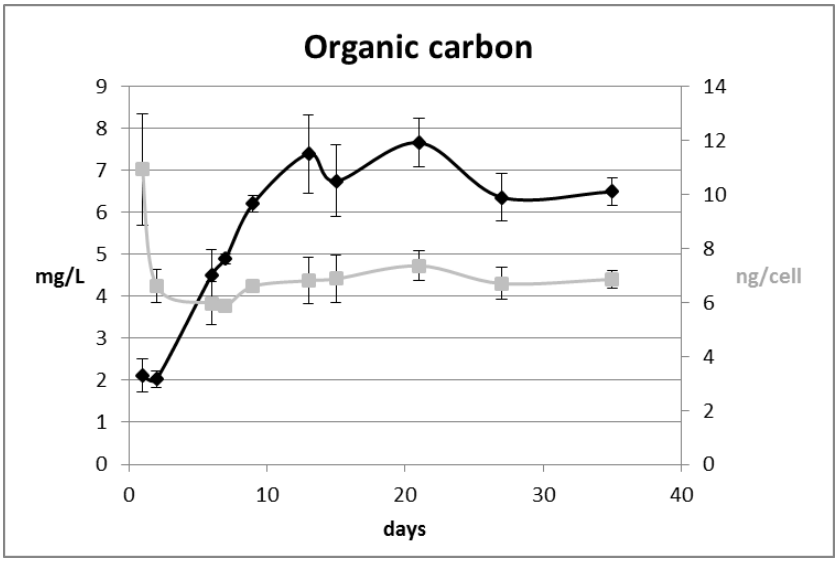

Figure 14. Here are reported the measures of organic carbon detected by CHN elemental analyzer, both expressed as mg/L (black profile) and ng/cell (gray profile).

The carbon detected by CHN elemental analyzer reached the maximal value of 7.65 mg/L at day 21. Carbon profile was generally in good agreement with the growth curve based on the cell number (Fig. 8), in fact the quantities of carbon per cell resulted constant excluding day 1 (see the

gray curve in Fig. 14), and also with daily mean cell dimensions (Fig. 9), contrary to what was observed in the second part of the experiment Alpha (see section 3.2.2).

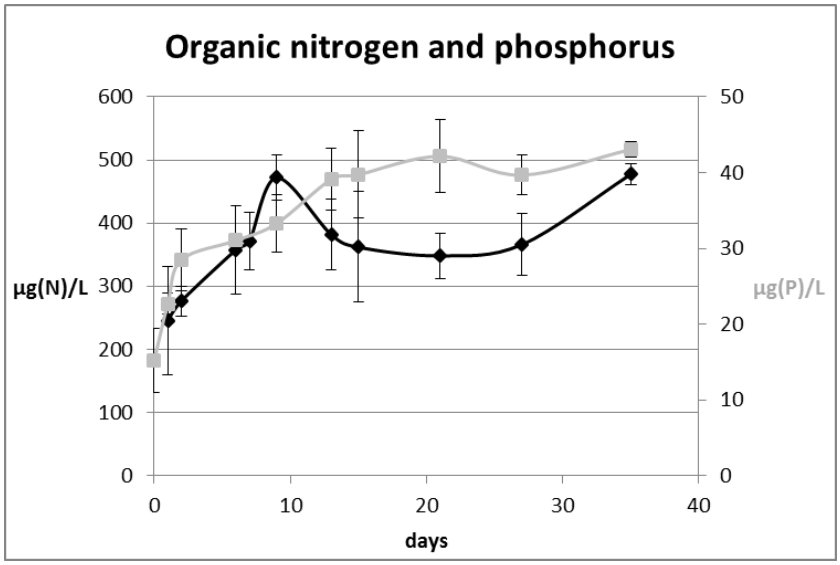

Figure 15. Profiles of organic nitrogen and phosphorus expressed as µg/L.

The amount of organic phosphorus (Fig. 15) increased rapidly in the first two days, after which its increase was slowed down for the rest of the experiment, while maintaining a stable trend. At the contrary in the experiment Alpha the trend of organic P in the late stationary phase took a decreasing trend (Pezzolesi et al., in prep.). As the initial inorganic phosphorus in the culture medium was completely depleted by day 7 (Fig. 11), we might assume that *O.* cf. *ovata* has continued to acquire phosphorus from organic matter thanks to its mixotrophic abilities (*O.* cf. *ovata*, as other dinoflagellates, is able to synthesize the enzyme "alkaline phosphatase"), or from the bacterial phosphorus pool because of its phagocytic abilities (Faust, 1998).

The profile of organic nitrogen can be divided in three parts. For the first part (days 0 - 9), the curve was in good agreement with the organic phosphorus' one: the amount of nitrogen in the cells increased quite rapidly. Instead in the second part (days 9 - 27) was observed an unexpected decrease in organic N and stabilization: it could be correlated to the parallel decline in chlorophyll (Fig. 10), since chlorophyll is an N-rich molecule, but it is more realistically associated to a decrease in the protein content of the cells, as already observed in the latter part of the experiment Alpha (Pezzolesi et al., in press). This could be a further proof of the aging of the cells and their entrance in a decaying phase in the last part of the experiment. Finally the second increase in organic N, observed in the third part of the curve (days 21 - 35), could be due to processes of bacterial remineralization (Tezuka, 1989) or, as seen for the phosphorus, to the

mixotrophic/phagocytic abilities of the alga. This second increment of N seems not to have influenced the synthesis of chlorophyll.

In the following Figure 16 are shown the cellular carbon to phosphorus and nitrogen molar ratios.

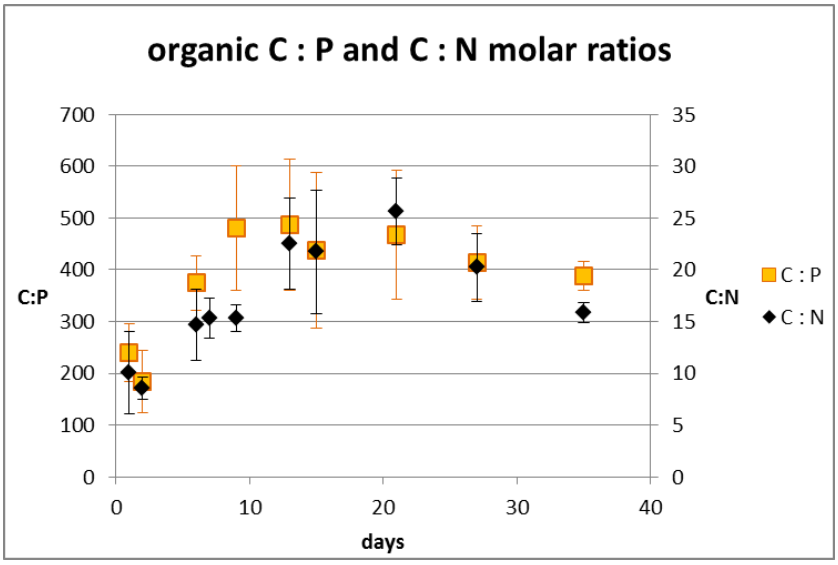

Figure 16. C:P (yellow spots) and C:N (black spots) organic molar ratios.

The C:P ratio had a similar trend to the C:N ratio, in fact both have increased from the beginning of the experiment, and reached the maximal values of 487 and 26 in the middle (day 13) and late (day 21) stationary phase, respectively, then decreasing both during the decaying phase. This first increasing and then decreasing trend of the C:P and C:N ratios during the exponential-stationary and decaying phases, respectively, led us to think that the maximum values achieved were the most extreme ones tolerable by the cells of *O.* cf. *ovata*. Then these maximum values have been adopted as limiting threshold-parameters for the alga in the modelling work.

Even if *O.* cf. *ovata* is a benthic dinoflagellate, the values of these ratios are extremely high when compared to those calculated by Redfield (1934, 1958) for marine phytoplankton, or C:P = 106 and C:N = 6.6. In literature there are only a few comparable examples for such high values. Vidyarathna & Granéli (2013) found some C:P ratios of 565 and 334 in a Tyrrhenian *O.* cf. *ovata* strain cultured in severe P-limitation at 20° C and 30° C, respectively, and a C:N ratio of 19.4 in the same strain cultured in a severe N-limitation at 20° C. Also another experiment conducted on the planktonic dinoflagellate *Alexandrium fundyense* revealed maximal values of C:P ratios around 350, for algae cultured in P-limitation at 18° C (John & Flynn, 2000).

4.1.6 Toxins

The HRLC-MS analyses that were conducted on the cell extracts revealed, in order of abundance, the presence of intra-cellular ovtx-a (55-65%), ovtx-b (25-30%), ovtx-d/e (10-15%), ovtx-c (3-5%), while the putative palytoxin was not detected, probably because below the limit of detection (LOD) of the instrument (Fig. 17). The analysis on the culture medium instead did not reveal the presence of any extra-cellular toxin, because toxin concentrations were below the LOD.

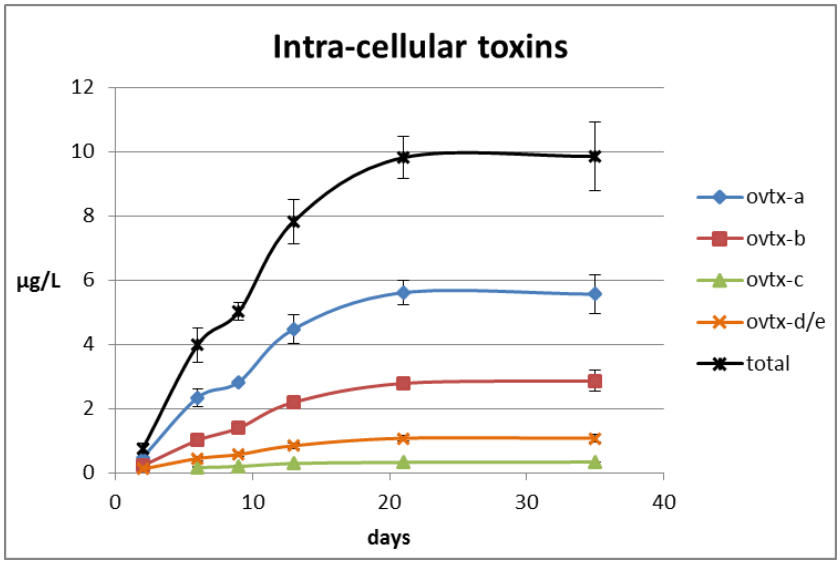

Figure 17. Concentration (as µg/L) of the various toxins, and their total amount.

Relative abundances of the different toxins were constant during the growth, as already observed in the exp. Alpha (Pezzolesi et al., in press) and in Ciminiello et al. (2011[b]), leading us to hypothesize that none of them can probably acts as precursor for the others.

It is very interesting how this dinoflagellate, if in nutrient-stress, continues to synthesize toxins and neglects the synthesis of chlorophyll, investing its resources more in the toxicity than in the growth. In the second part of the experiment the concentration of the toxins even exceeds that of chlorophyll-a, as shown in Figure 18.

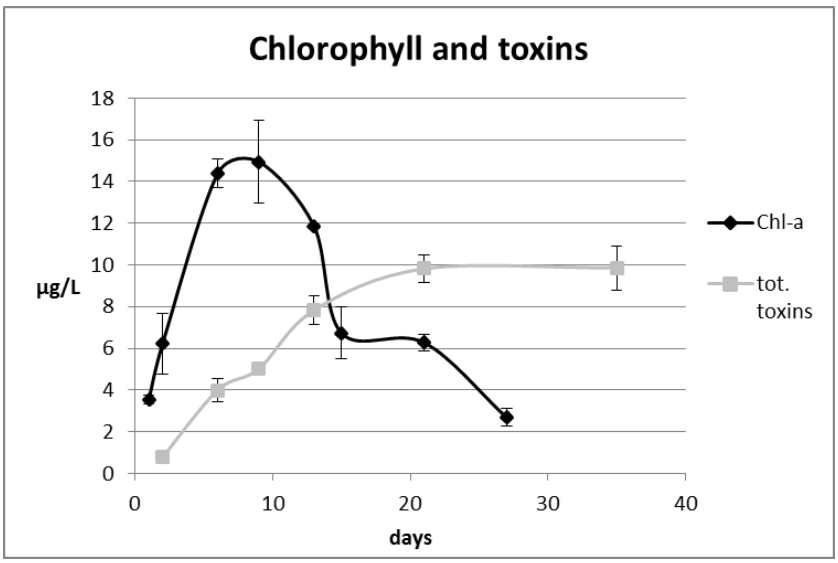

Figure 18. Comparison of the trends of chlorophyll-a and total toxins, both expressed as µg/L.

In the light of this result, we could hypothesize that *O.* cf. *ovata* may be able to change feeding strategy if in very stressful conditions, moving from a predominantly autotrophic strategy (with high metabolic costs and demand for nutrients) to an opportunistic and less active one, capable of mixotrophy and defense from grazing through the production of toxins, which apparently maintains in any case.

4.1.7 Growth curve and cell volume of bacteria

The bacterial growth resulted constant since the first day of the experiment (Figure 19) and appeared not closely related, at least in the 35 day-period of the experiment, to the number of *O.* cf. *ovata* cells or their total biomass.

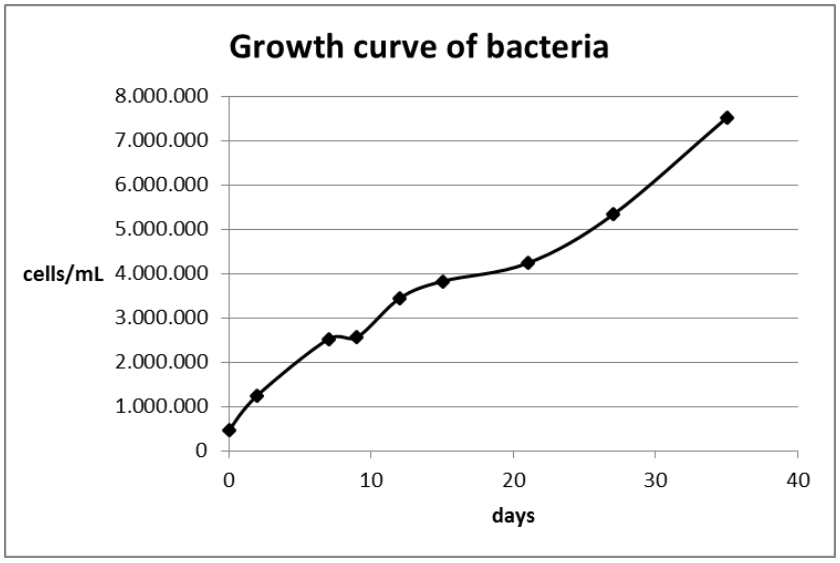

Figure 19. Bacterial growth expressed as cells per mL.

Anyway the influence of bacteria on *O*. cf. *ovata* growth dynamics should be relevant considering their elevate number in the cultures (or in nature, as well).

Relating to marine microalgae in general, bacteria could be competitors for inorganic nutrients during the exponential phase (Azam et al., 1983; Bratbak, 1987; Jürgens & Güde, 1990), producers of inhibitory or stimulatory compounds, degraders of algal toxins (Donovan et al., 2009; Green et al., 2010 and references therein), useful allies in the stationary phase because of the ability of some to remineralize nutrients from organic matter or also, in this particular case, some potential prey for the alga (Faust, 1998). An experiment on the bacterial influence on *O.* cf. *ovata* was conducted by Vanucci et al. (2012[a]): an Adriatic strain was cultured in axenic conditions (without bacteria) and in ordinary culture conditions, and it was observed that the removal of bacteria unaffected algal growth except for conferring a more steady stationary phase with a lower cell toxins and an higher extra-cellular toxins concentration, changes however though not significantly. Given the importance of the topic, further studies would be needed.

4.2 Findings from experiments Alpha and Beta

4.2.1 O. cf. *ovata tolerance to nutrient deficiency-stress*

O. cf. *ovata* is able to grow in extremely stressing conditions with respect to internal nutrient quotas, as evidenced from the experiments Alpha and Beta, and also from the study of Vidyarathna & Granéli (2013), conducted on a Tyrrhenian strain of this species. Intra-cellular carbon to nutrient molar ratios from the two experiments Alpha and Beta are reported in Table 7.
The highest value of C:P ratio (601) was detected in the experiment Alpha at day 35, and the highest C:N ratio (27.1) in the same experiment at day 27, while the highest N:P ratio (31) was observed in the exp. Beta at day 9.

day	exp. Alpha			exp. Beta		
	C:P	*C:N*	*N:P*	*C:P*	*C:N*	*N:P*
1	-	-	-	240	10	24
2	-	-	-	183	8,7	21
3	**97**	**7,5**	**13**	-	-	-
5	102	7,3	14	-	-	-
6	**124**	**7,3**	**17**	374	15	25
7	144	6,9	21	**397**	**15,3**	**26**
9	153	7	22	480	15,5	31
12	194	11	17	-	-	-
13	-	-	-	487	22,1	22
15	197	14,1	14	437	21,9	20
21	318	21,2	15	468	26	18
27	406	27,1	15	413	20,7	20
35	601	25	24	388	15,5	25
Redfield	106	6,6	16	106	6,6	16

Table 7. Internal C:P - C:N - N:P mean molar ratios in *O*. cf. *ovata* cells which were detected in the two experiments Alpha and Beta, compared to those calculated from the Redfield molar proportion C:N:P of 106:16:1 for marine phytoplankton. Values in **bold type** are the result of interpolations and not of direct measurements.

During the exponential phase (day 1-9) of the experiment Alpha, in which there was a large availability of nutrients in the culture medium, we observed a balanced growth in terms of intra-cellular nutrient quota: *O*. cf. *ovata* cells maintained for 9 days some C:P and C:N ratios that were close to the Redfield ones (Table 7). Also the cells of the experiment Beta, which started from

already unbalanced conditions (C:P=240, C:N=10, N:P=24 at day 1) because of the acclimation before the experiment, probably tried to reach the Redfield ratio during the short exponential phase. In fact the various ratios decreased from day 2 to day 1, but were not able to reach Redfield values probably due to the a few inorganic nutrients available. This confirms that presumably *O*. cf. *ovata* grows tending to the Redfield ratio if there are enough nutrients in the medium.

In the stationary phases of the experiments Alpha and Beta (day 9-35 and 7-21, respectively) it was observed a large accumulation of organic carbon (mostly preserved in the decaying phase of the experiment Beta, day 21-35) which unbalanced the C:P and C:N ratios to very high values, up to five and four times the Redfield ratio, respectively (Table 7). The N:P ratios seemed to be the less variable compared to the C:P and C:N ones, increasing to a maximum value that is only twice the Redfield ratio: this could be a sign of lower physiological tolerance of *O*. cf. *ovata* to the unbalance between these two nutrients in its cell.

A consequence of nutrient deficiency coupled to the increase of organic carbon was the lowering of the chlorophyll to carbon weight ratios to very low levels in both experiments Alpha and Beta, with minimum values of 0.0028 and 0.0004 at days 21 and 27, respectively (Fig. 20).

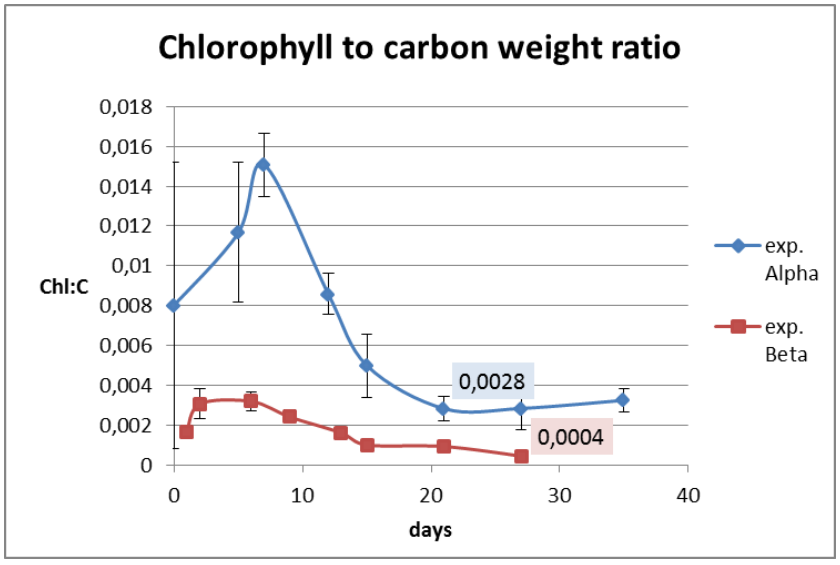

Figure 20. Trends of the chlorophyll to carbon weight ratios for *O*. cf. *ovata* in the two experiments. The carbon used to calculate the ratios was taken from the processed organic carbon values, described in section 3.2.2 and 4.2.3.

In the light of these results, we proposed some mechanistic hypothesis in order to explain the observed trends of the algal variables carbon, nitrogen, phosphorus and chlorophyll-a in nutrient-stress condition, as briefly mentioned in the section 2. These assumptions were materialized as changes in the ERSEM equations and parameters (see section 3.3.3), and finally have been tested

through simulations of the latter, trying to reproduce the various dynamics observed in the two experiments Alpha and Beta. These assumptions are again listed here:

- ***O.* cf. *ovata* strongly reduces chlorophyll synthesis when stressed by nutrient**, concomitantly with the enhanced production of toxins
- ***O.* cf. *ovata* is able to reduce its metabolism (forming a sort of resting stage)** under extreme nutrient limiting condition. The accumulation of cellular carbon and toxins with respect to nutrient and chlorophyll is part of this strategy.

4.2.2 O. cf. *Ovata toxicity*

As mentioned in the section 3.3.2, we found significant linear correlations between toxins to carbon intra-cellular ratios and both phosphorus to carbon and nitrogen to carbon intra-cellular ratios in the experiment Alpha (r = - 0.85 and r = - 0.79 respectively), as showed in Figure 21.
For the experiment Beta this correlation was not clear, but only because *O.* cf. *ovata* P:C and N:C ratios were very low since the beginning of the experiment and reached rapidly some values (0.0028 and 0.066 at day 6, respectively) that were quite close to the observed minimums (0.0021 and 0.038 at day 13 and 21, respectively).

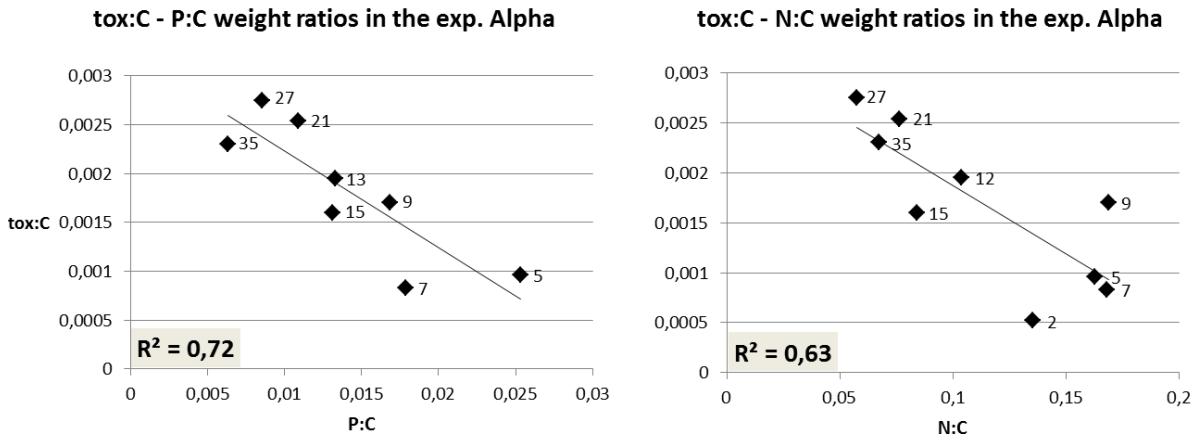

Figure 21. Toxins to carbon and nutrient to carbon weight ratios observed in *O.* cf. *ovata* cells in the experiment Alpha. Numbers close to the points represents the days of the experiment.

This correlation means that a decline of P:C and N:C ratios, due to an ongoing primary production coupled with poor nutrient conditions, as well as to an increase of intra-cellular nutrient stress, corresponded an increase in toxins' production (increasing tox:C ratio).

Thus we further formulated the following hypothesis, to be tested through modelling (see section 2 and 3.3.2): **toxin production**, which however continues to a low basal level in function of algal biomass, could be additionally **stimulated by increasing nutrient-stress condition** of the alga.

4.2.3 Results from the processing to organic carbon values

Because of the possible error in the cellular carbon detection by the CHN analyzer in samples from the last part (21-27-35) of the experiments Alpha and Beta, we decided to recalculate (for both the experiments) the POC values of those days according to the method which has been previously explained in detail in the section 3.2.2.

The relationships between the total cell volume and the carbon values from CHN (for the first 15 day of cultures) in both the experiments is showed in Figure 22, while the "definitive" curves of *O.* cf. *ovata* carbon, which have been considered in the modelling work, are reported in Figure 23.

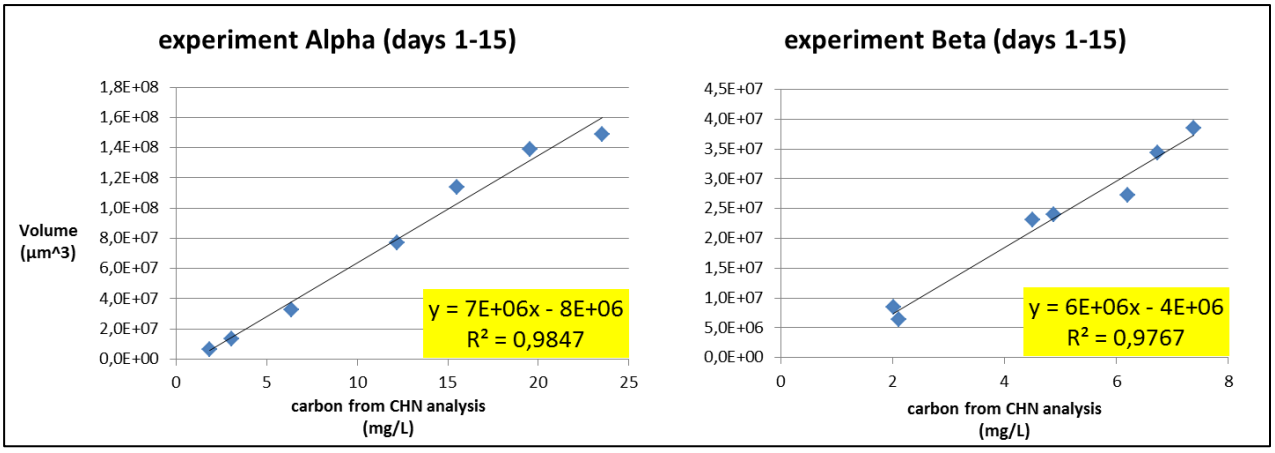

Figure 22. Relationship between total cell volumes and POC detected by the CHN analyzer. Equations of the regression lines and the correlation values are given in yellow field.

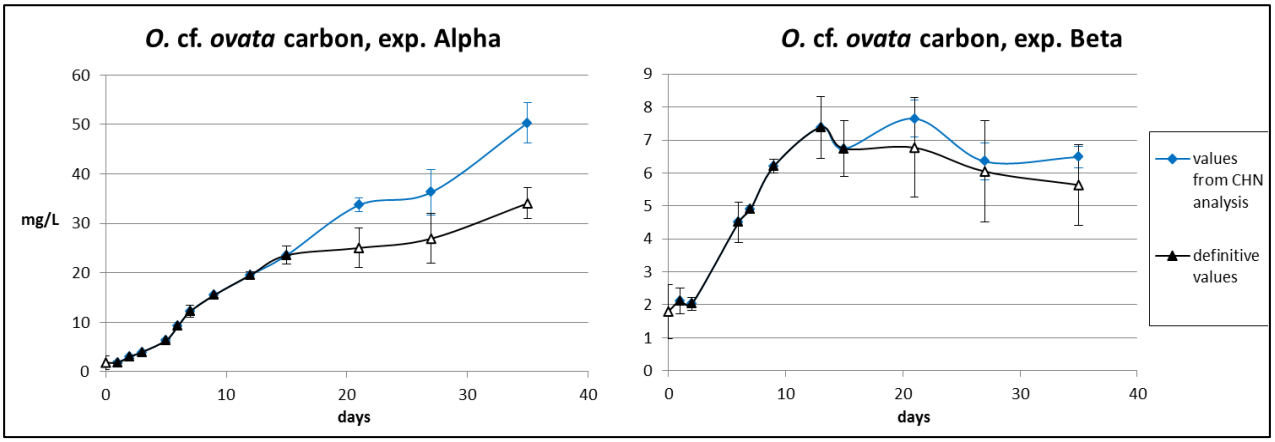

Figure 23. Profiles of cellular carbon in both experiments: the empty points represent the re-calculated values.

Just a suggestion for future studies on this dinoflagellate: in order to avoid, or limit, the inclusion of mucilage and bacteria in the samples to be allocated in the CHN analyzer, one might filter the culture samples with high porosity filters (for example, 1.2 mm), however sufficient to hold all the algal cells, and perhaps further rinse the sample-filter by filtering some synthetic seawater.

4.3 Simulating the experiment Alpha

4.3.1 A first run of ERSEM

The first modelling experiment was to run ERSEM with the set-up described in section 3.3.1 but without any change in the source code and in the parameters set, obtaining a 40 days-simulation output which is summarized through the trends of some chosen variables in Figure 24.

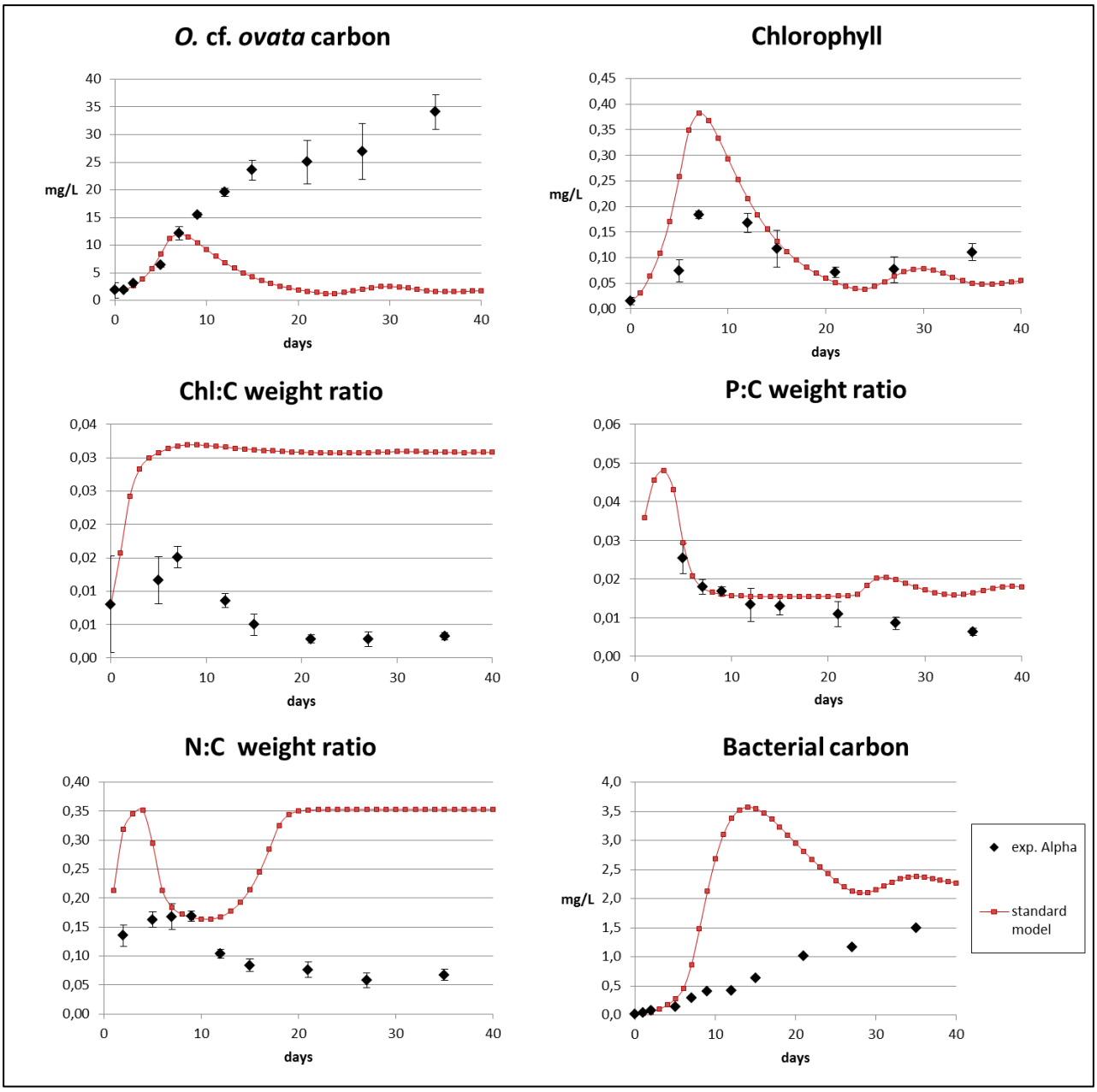

Figure 24. Here are compared the experimental values of some variables with those obtained from the first simulation of the experiment Alpha, which used the standard set of equations and parameters for the phytoplanktonic functional group of dinoflagellate (P4; Blackford et al., 2004).

The analysis of simulations clearly showed that the model, with the standard set of equations and parameters for the planktonic functional group of dinoflagellates, was not able to reproduce the trends of the experiment Alpha.

4.3.2 Results of the modelling work

The second step of the modelling work was to modify the model formulation following the assumptions on the physiology of *O.* cf. *ovata* we made on the basis of the experimental results (see sections 4.2.1 - 4.2.2). In this phase of the work, the model was largely modified in terms of both source code (i.e. the fundamental equations) and parameters. All the alterations and additions to the standard model equations are summarized in the sections 3.3.2 -3 -4 of this thesis. Model parameters (Table 6) were manually tuned to obtain a better fit with the observed data.

The modified model was able to reproduce many of the trends observed in the experiment Alpha (Fig. 25), including the production of toxins (Fig. 26).

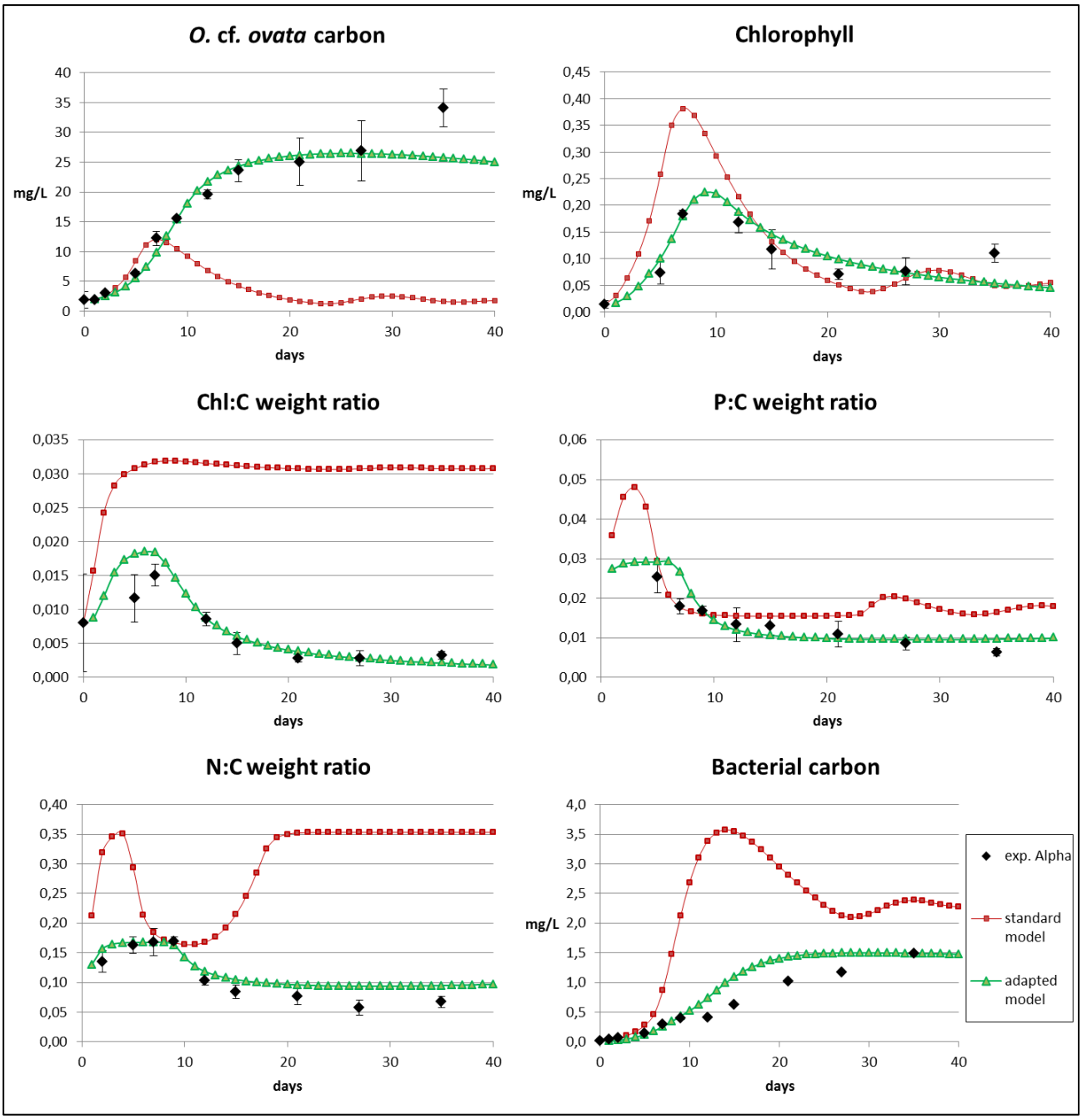

Figure 25. Some charts comparing the definitive simulation (in green) of the experiment Alpha, obtained after the updates in the source code and in the parameters, with the first simulation (in red) operated through the standard model (Fig. 24), and the values from exp. Alpha.

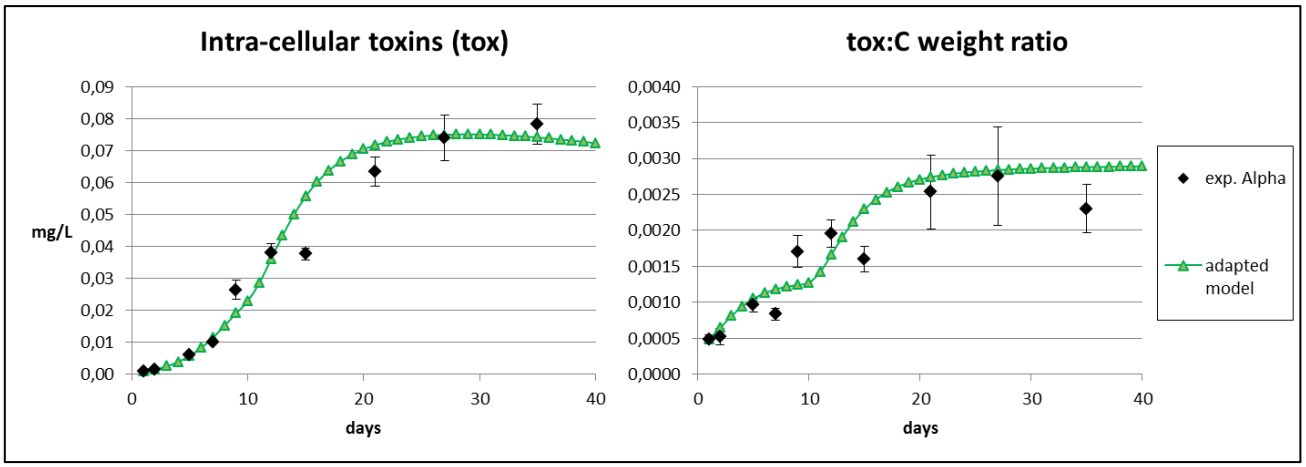

Figure 26. Here are displayed the trends of the two new variables "tox" and "tox/C" that were introduced in the model, compared to the toxins' trends observed in the exp. Alpha. Experimental toxins were processed as only the carbon fraction of the "ideal" toxin, which represents for the total weight of all the toxic species (see section 3.2.2).

All the model-trends reported in Figures 25 and 26 were in good agreement with the experimental data, as highlighted by the statistic indices reported in table 8. The correlation between modeled and observed variables was in all cases very high, indicating an excellent qualitative agreement. The capacity of the model to reproduce the "quantity" of the observed variables was good, as evident from the mean percentage error which was well below the 20% in 7 variables over 8.

STATISTIC	*O. cf. ovata* carbon	Chlorophyll	Chl : C weight ratio	P : C weight ratio	N : C weight ratio	Bacterial carbon	Intra-cellular toxins (tox)	tox : C weight ratio
Pearson correlation (r)	0,965	0,808	0,968	0,904	0,986	0,951	0,975	0,924
P-value	< 0,001	0,028	< 0,001	0,002	< 0,001	< 0,001	< 0,001	< 0,001
Root mean square error	2,86 mg/L	0,029 mg/L	0,0028	0,0037	0,02	0,25 mg/L	0,0069 mg/L	0,0004
Mean percentage error	-4,9%	8,1%	13,7%	11,1%	20,5%	7,9%	4,6%	11,5%

Table 8. Results of the statistic calculations on eight variables, performed to test the goodness of the simulation of the adapted model in reproducing the experiment Alpha.

The p values associated to the Pearson correlation were very low ($p < 0.01$), indicating that the correlation is highly significant) except for the variable "chlorophyll", for which the p-value was 0.028. This flaw is primarily due to the inability of the model to reproduce the last part (day 27-35) of the chlorophyll experimental trend: in fact in the last phase of the exp. Alpha was observed a second moderate increase of chlorophyll-a (Pezzolesi et al., in press) that has been left unexplained in this work, since it was not followed by an increase of cellular nutrients.

Overall these results allow us to support our starting hypotheses about *O*. cf. *ovata* which stated that:

1) the production of toxic compound is stimulated by the cellular nutrient deficiency (or nutrient-stress)
2) the chlorophyll synthesis is heavily controlled by intracellular nutrient level
3) the metabolic rate is lowered in condition of nutrient-stress. The reduction in carbon losses leads to an extremely high carbon to nutrient and carbon to chlorophyll ratios. This behavior could be part of a metabolic strategy aimed to maximize defense mechanisms (toxins and accumulation of carbon) at the expenditure of growth efficiency (chlorophyll and balanced internal stoichiometry).

4.3.3 Sensitivity tests

During the modelling work, we also performed some sensitivity analyses in order to evaluate the importance of specific processes (and single parameters) on the model capacity to simulate the experiment Alpha. More specifically, we performed sensitivity analyses on respiration, mortality and bacteria related dynamics.

RESPIRATION (METABOLISM)

In order to evaluate to what extent the model was "sensitive" to the respiration process (formulated as described in section 3.3.3) and relative parameters, the model was run with the following configurations:

- with $\mathbf{NS}^{res}$ and a $r_{R.res} = 0.002$
- with $\mathbf{NS}^{res}$ and a $r_{R.res} = 0.05$
- without $\mathbf{NS}^{res}$ and a $r_{R.res} = 0.01$

Results of these simulations compared with experimental data are shown in figure 27.

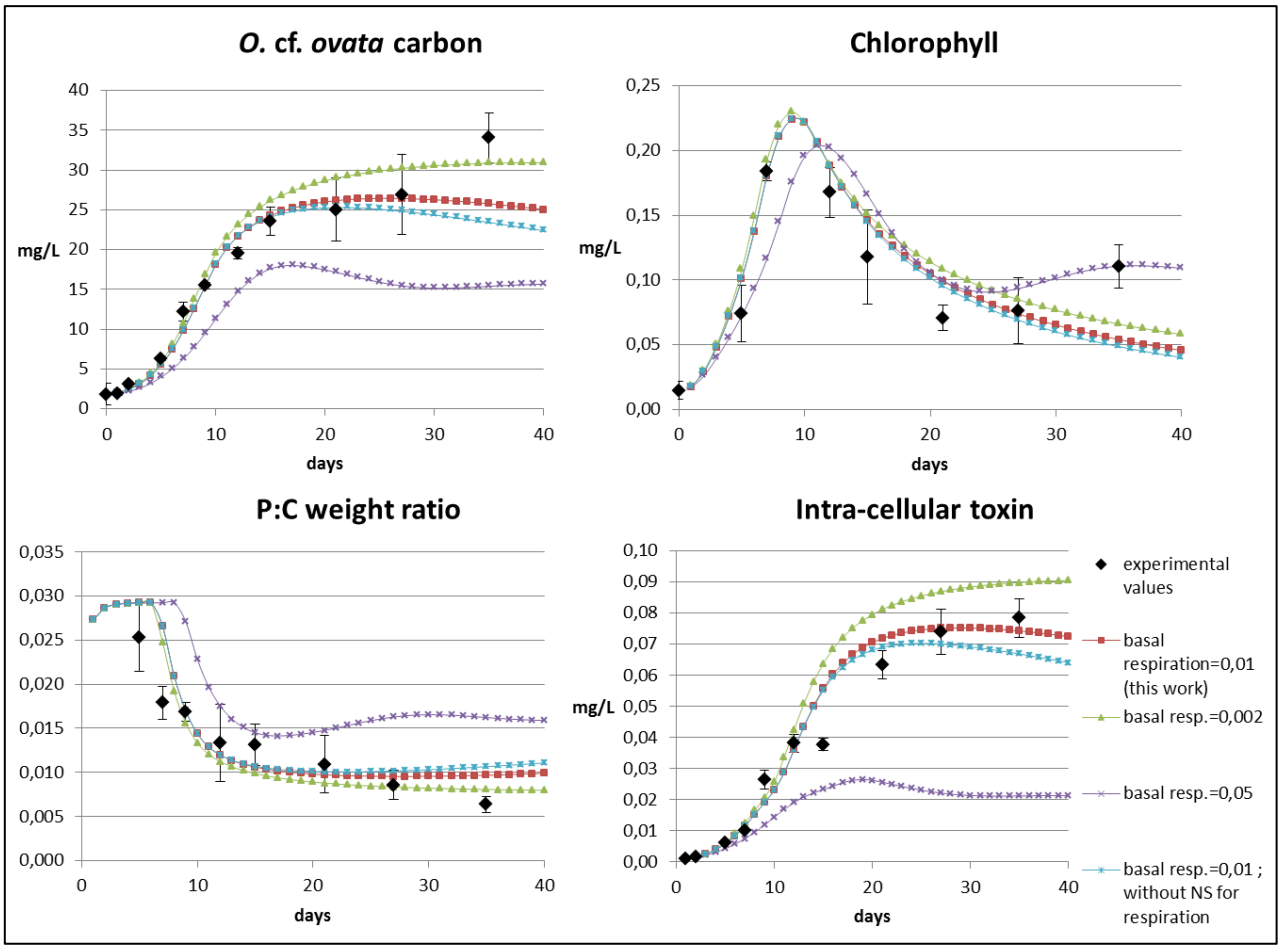

Figure 27. Simulations with different model settings in order to test the influence of the limiting factor $\mathbf{NS}^{res}$ and the parameter $\mathbf{r_{R.res}}$ on the studied dynamics.

From these sensitivity tests emerged that the parameter $r_{R.res}$ was highly influent on the growth dynamics of the alga. The factor $\mathbf{NS}^{res}$ was (as expected) less relevant in the first phase of the experiment but important in improving the qualitative agreement in the last days of the experiment.

MORTALITY

Furthermore, in order to evaluate to what extent the model was "sensitive" to the mortality (formulated as described in section 3.3.3), the model was run with the following configurations:

- without $\frac{\mathbf{1}}{(\mathbf{NS+0,1})}$ and a $r_{lys} = 0$
- without $\frac{\mathbf{1}}{(\mathbf{NS+0,1})}$ and a $r_{lys} = 0.05$
- with $\frac{\mathbf{1}}{(\mathbf{NS+0,1})}$ and a $r_{lys} = 0.005$

From these tests, the parameter r_{lys} resulted to be relevant in influencing the algal growth (especially in terms of quantity). The decoupling of mortality from nutrient stress had an high influence on the quality of simulations, by helping us to reproduce the last phase of the experiment (as previously said for the metabolism-respiration).

BACTERIA

We also run ERSEM without the functional group of bacteria, in order to test the bacterial influence on algal growth dynamics. The differences between the simulations with and without bacteria were very small and this suggests that bacteria, although competing with *O*. cf. *ovata*, for dissolved nutrients, do not play a crucial role in the dynamics observed in the experiments.

4.4 Simulating the experiment Beta

4.4.1 The simulation and its gaps

After being able to reproduce the dynamics of the experiment Alpha, the model was also used to simulate the experiment Beta. To this end, we initialized the model with values observed at the beginning of the experiment Beta.

Model results are summarized in Figure 28.

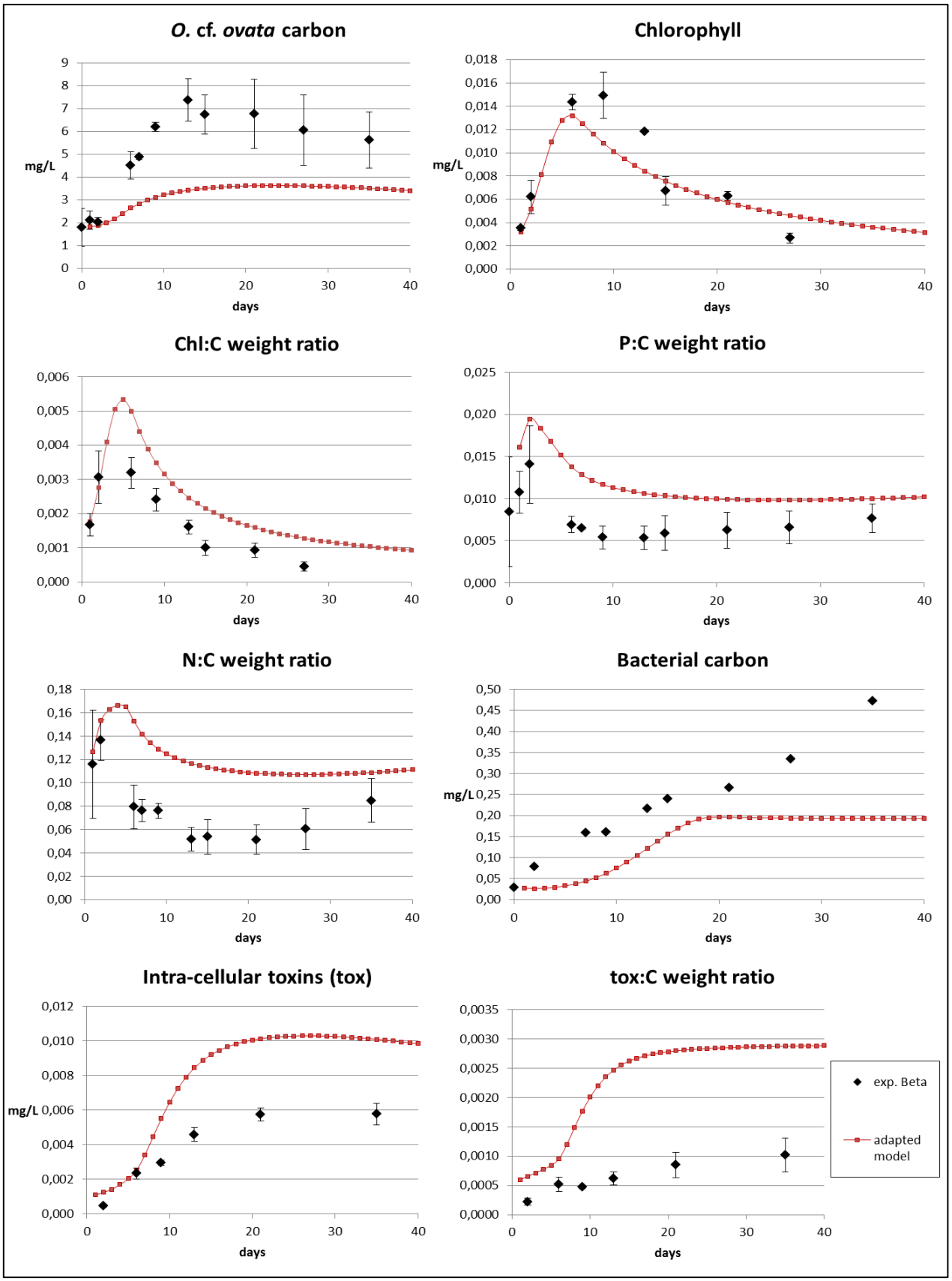

Figure 28. Some charts comparing the simulation of the experiment Beta (in red), obtained through the adapted model (already used for the exp. Alpha), and the values observed in the exp. Beta.

The simulation was quite good from a qualitative point of view, as highlighted by the Pearson correlations and relative p values, reported in Table 9. For seven of the eight considered variables the correlations were above the value of 0.84, and only the correlation for the N:C weight ratio (0.62, p value = 0.054) was lower of this value.

STATISTIC	*O. cf. ovata* carbon	Chlorophyll	Chl : C weight ratio	P : C weight ratio	N : C weight ratio	Bacterial carbon	Intra-cellular toxins (tox)	tox : C weight ratio
Pearson correlation (r)	0,95	0,93	0,84	0,89	0,62	0,86	0,98	0,89
P-value	< 0,001	< 0,001	0,009	< 0,001	0,054	0,007	< 0,001	0,017
Root mean square error	2,53 mg/L	0,002 mg/L	0,001	0,005	0,052	0,134 mg/L	0,003 mg/L	0,001
Mean percentage error	-38,1%	-1,8%	65,7%	63,7%	72%	-50,7%	84,2%	211%

Table 9. Results of the statistic calculations on eight variables, performed to test the goodness of the simulation of the adapted model in reproducing the experiment Beta.

Nevertheless, the model has not been able to reproduce the experimental trends in terms of quantity, as can be clearly seen from the charts (Fig. 28) and from the Mean Percentage Errors (MPEs) reported in the previous table: in particular the model-alga did not grow enough (see the chart of cellular carbon) as was observed in reality for *O.* cf. *ovata* during the exp. Beta. This lack of carbon has then been quantitatively felt by the other model variables.

4.4.2 Possible explanations of gaps and further changes to the model

In order to study the behavior of an organism subjected to different treatments would be useful to have a common starting point to be used as a reference.

It should be noted that the starting status of the dinoflagellate at the beginning of the two experiments was not equal. For example, the stoichiometric compositions of the algae at the beginning of the two experiments were remarkably different (see Table 7 in section 4.2.1). We argue that these differences were due to the different nutrient conditions to which the algae were acclimated and have possibly affected the algal metabolisms in the experiments.

We hypothesized therefore that the inability of the model in reproducing the growth trend of the cellular carbon of the experiment Beta, was due to the lack of such acclimation processes in the model itself. Acclimation to given environmental conditions (e.g. light, nutrients mixing etc.), in fact, may strongly affect cellular metabolism in almost all its aspects (Morel, 1987; Smith et al., 1992; Geider et al., 1998).

In other words, the relatively high net primary production observed in the experiment Beta, could be due to the fact that *O.* cf. *ovata* was physiologically adapted to nutrient-stress conditions since the beginning of the experiment. For this reason, the level of stress induced by nutrient limitation in the experiment Beta was lower than in the experiment Alpha where the cells were acclimated to higher nutrient conditions. In order to provide a preliminary assessment of this hypothesis we manually tuned model parameters regulating the stress-threshold of nutrient limitation. Model parameters tuned for this experiment are reported in the section 3.3.4.

Model results for this experiment are summarized in Figure 29 and Table 10.

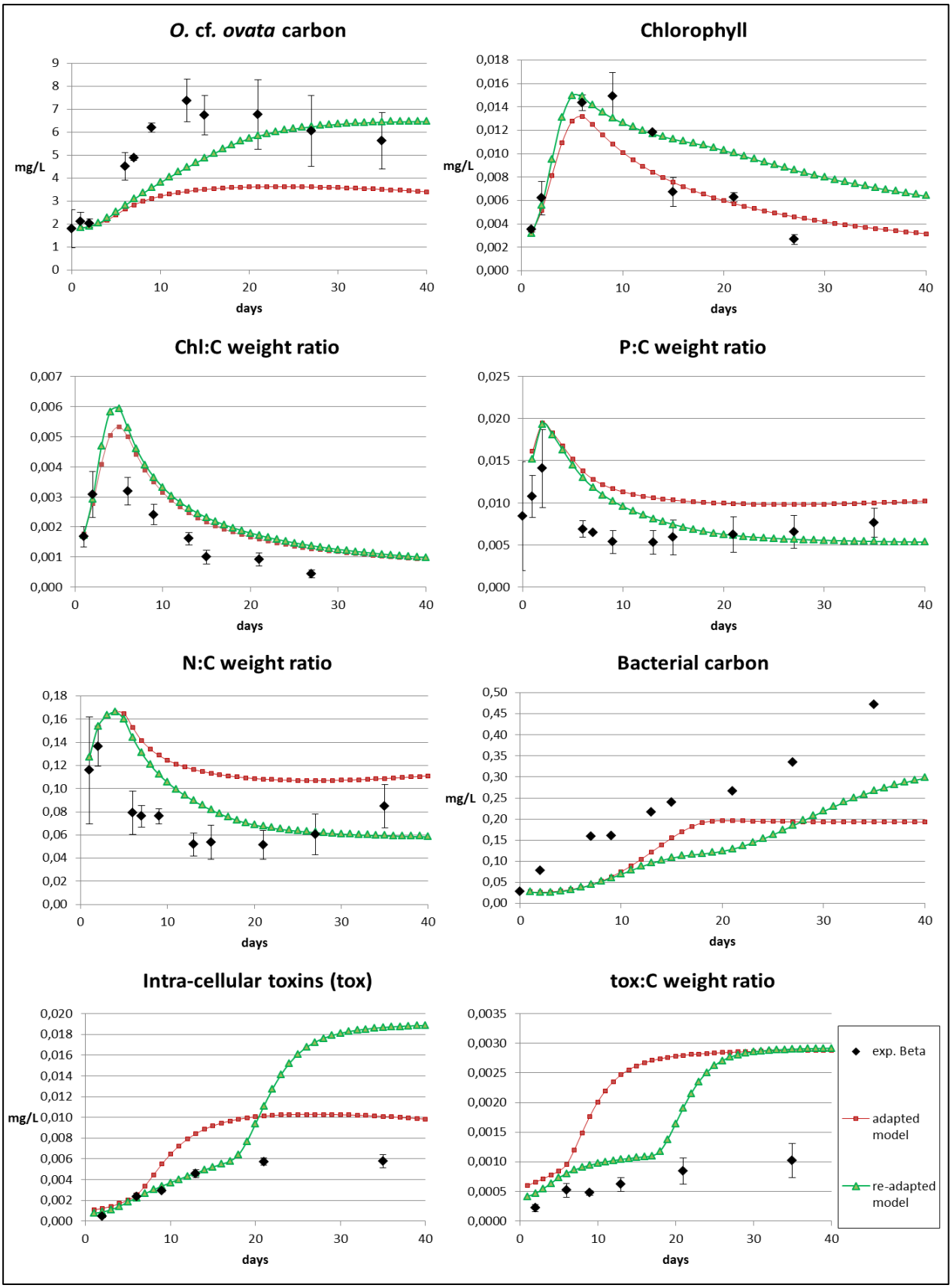

Figure 29. Comparison between the exp. Beta values, the simulation showed previously in Figure 28 (in red), and the last simulation through the re-adapted model.

STATISTIC	*O. cf. ovata* carbon	Chlorophyll	Chl : C weight ratio	P : C weight ratio	N : C weight ratio	Bacterial carbon	Intra-cellular toxins (tox)	tox : C weight ratio
Pearson correlation (r)	0,76	0,80	0,83	0,79	0,68	0,99	0,83	0,95
P-value	0,01	0,017	0,01	0,007	0,031	< 0,001	0,041	0,003
Root mean square error	1,64 mg/L	0,003 mg/L	0,001	0,004	0,035	0,13 mg/L	0,006 mg/L	0,001
Mean percentage error	-20,2%	39,3%	75,9%	37,6%	35%	-56,8%	71,1%	107%

Table 10. Results of the statistic calculations on eight variables, performed to test the goodness of the simulation of the re-adapted model in reproducing the experiment Beta.

The results of this experiment are controversial. From one side, the model seems to slightly improve its skills by reducing the mismatch between simulations and observations in terms of quantity (see MPEs in Tab. 10); from the other, model performance loses a bit in terms of qualitative agreement with the observed data (see Pearson correlations and relative p values in Tab. 10).

For this reason, is not possible to draw any meaningful conclusion on this particular aspect of the work. However, although preliminary, our results strongly strengthens the case for further experiments specifically designed to investigate the capacity of *O.* cf. *ovata* to acclimate to different nutrient regimes. Such experiments will give new insights on the metabolism of this peculiar organism helping to understand his capacity to successfully grow under adverse environmental conditions and produce toxins. These experiments should be used to further refine the presented numerical model making it an even more powerful investigative tool.

5. CONCLUSIONS

The combined experimental and modelling study applied in this thesis represents a new approach on the study of the benthic dinoflagellate *Ostreopsis* cf. *ovata*. In particular, the experiment Beta presented in this thesis, conducted on an *O.* cf. *ovata* Adriatic strain, has enabled us to increase our knowledge on this toxic species: the results obtained have confirmed some physiological aspects of this dinoflagellate that were already emerged from the previous experiment Alpha (Pezzolesi et al., in press; Pezzolesi et al., in prep.), but also improved the physiological dataset on *O.* cf *ovata*. More specifically, in this experiment emerged that *O.* cf. *ovata* is able to grow in situations of severe internal nutrient-stress, reaching maximum C:P and C:N intracellular molar ratios of 487 and 26, respectively, which are very far from the values of 106 and 6.6 proposed by Redfield (1934, 1958) as optimal mean values for marine phytoplankton in general. Furthermore *O.* cf. *ovata* reached very low chlorophyll-a to carbon cellular ratios, all below the value of 0.004 throughout the experiment and with a minimum value of 0.0004, which are not compatible to the Chl-a:C values observed in cultured marine microalgae usually ranging from 0.1 to 0.01 (Geider 1987, 1993); nevertheless it continued to maintain a positive (day 0-13) or balanced (day 13-21) net primary production in the first and mid- part of the cultures, and also to produce high molecular weight toxins requiring elevate metabolic cost. A significant inverse relationships between cellular toxin to carbon ratio and both phosphorus and nitrogen to carbon ratio was also observed in the experiment Alpha.

In the light of these findings, we hypothesized 4 physiological processes directly associated with an increasing state of intra-cellular nutrient-stress (increase of C:P and C:N cellular ratio): i) a stimulation of toxin production, ii) a strong decrease in chlorophyll synthesis, iii) a reduction of metabolic rates, iv) a reduction in mortality rate possibly due to the ability to form resting stage.

The newly developed version of ERSEM we have used was able to accurately reproduce many of the trends observed in the experiment Alpha, and this supports our starting hypotheses. Nevertheless, the simulation of the experiment Beta was not equally good and this highlights that some mechanisms governing *O.* cf. *ovata* growth and toxin production are still missing in our model. One possible explanation of the inability of the model to reproduce the experiment Beta is the lack of acclimation processes in the model, since the algae of the experiment Beta have previously been acclimated to different (more limiting) nutrient conditions with respect to the experiment Alpha.

Further experiment purposely focused to study the capacity of *O*. cf. *ovata* to acclimate to different nutrient conditions are required to shade light on this particular aspect. Outcomes from such experiments will provide additional informations to further develop the presented model and to definitively validate the proposed hypotheses.

ACKNOWLEDGEMENTS

Firstly I would like to thank the people who have in some way participated in this thesis, for the opportunity and trust they have given me, for practical help, for patience, for guiding me when there was need, or even simply for having expressed an interest: the Professors Rossella Pistocchi and Silvana Vanucci, my dear tutors Dr. Laura Pezzolesi and Dr. Luca Polimene, Dr. Franca Guerrini.

I also thank the "colleagues" of the PML for the moral and practical help, and for making me feel almost at home: Stefano Ciavatta, Yuri Grisendi, Giorgio Dall'Olmo, Laura Ruffoni, Marie-Fanny Racault, Lee De Mora, Momme Butenschön, Stephane Saux Picart, Gianfranco Anastasi, and all the others.

I am also grateful to those few friends who made Ravenna a livable city.

Finally, I am grateful to my parents Rosaria and Massimo for the support they have always given me, and for believing in me, allowing me to study what I liked most. Thanks…

REFERENCES

Accoroni S., Romagnoli T., Colombo F., Pennesi C., Di Camillo C. G., Marini M., Battocchi C., Ciminiello P., Dell'Aversano C., Dello Iacovo E., Fattorusso E., Tartaglione L., Penna A., Totti C. (2011). *Ostreopsis* cf. *ovata* bloom in the northern Adriatic Sea during summer 2009: ecology, molecular characterization and toxin profile. *Marine Pollution Bulletin*, 62 (11): 2512-2519.

Accoroni S., Romagnoli T., Pichierri S., Colombo F., Totti C. (2012). Morphometric analysis of *Ostreopsis* cf. *ovata* cells in relation to environmental conditions and bloom phases. *Harmful Algae*, 19: 15-22.

Aikman K. E., Tindall D. R., Morton S. L. (1993). Physiology and potency of the dinoflagellate *Prorocentrum hoffmannianum* during one complete growth cycle. In: T. J. Smayda, Y. Shimizu (Eds.), *Toxic Phytoplankton Blooms in the Sea*, Elsevier, Amsterdam, Netherland. pp. 463-468.

Alcala A. C., Alcala L. C., Garth J. S., Yasumura D., Yasumoto T. (1988). Human fatality due to ingestion of the crab *Demania reynaudii* that contained a palytoxin-like toxin. *Toxicon*, 26: 105-107.

Aligizaki K. & Nikolaidis G. (2006). The presence of the potentially toxic genera *Ostreopsis* and *Coolia* (Dinophyceae) in the North Aegean Sea, Greece. *Harmful Algae*, 5: 717-730.

Allen J. I., Somerfield P. J., Siddorn J. (2002). Primary and bacterial production in the Mediterranean Sea: a modelling study. *Journal of Marine Systems*, 33: 473-495.

Anderson D. M., Glibert P. M., Burkholder J. M. (2002). Harmful Algal Blooms and eutrophication: nutrient sources, composition, and consequences. *Estuaries*, 25 (4b): 704-726.

Artioli Y., Blackford J. C., Butenschön M., Holt J. T., Wakelin S. L., Thomas H., Allen J. (2012). The carbonate system in the North Sea: Sensitivity and model validation. *Journal of Marine Systems*, 102: 1-13.

Artioli Y., Blackford J. C., Nondal G., Bellerby R. G. J., Wakelin S. L., Holt J. T., Allen J. I. (2013). Heterogeneity of impacts of high CO_2 on the North Western European Shelf. *Biogeosciences Discussions*, 10 (6): 9389-9413.

Azam F., Fenchel T., Field J. G., Gray J. S., Meyer-Reil L. A., Thingstad F. (1983). The ecological role of water-column microbes in the sea. *Marine ecology progress series. Oldendorf*, 10 (3): 257-263.

Baretta J. W. & Ruardij P. (1988). Tidal flat estuaries: simulation and analysis of the Ems estuary. *Ecological Studies* (71). Springer Verlag, Heidelberg, Berlin, Germany. pp. 1-353.

Baretta J., Ebenhöh W., Ruardij P. (1995). The European Regional Seas Ecosystem Model, a complex marine ecosystem model. *Journal of Sea Research*, 33 (3-4): 233-246.

Baretta-Bekker J., Baretta J. W., Ebenhöh W. (1997). Microbial dynamics in the Marine Ecosystem model ERSEM II with decoupled carbon assimilation and nutrient uptake. *Journal of Sea Research*, 38 (3-4): 195-212.

Barroso García P., Rueda de la Puerta P., Parrón Carreño T., Marín Martínez P., Guillén Enríquez J. (2008). Brote con síntomas respiratorios en la provincia de Almería por una posible exposición a microalgas tóxicas. *Gaceta Sanitaria*, 22: 578-584.

Battocchi C., Totti C., Vila M., Masó M., Capellacci S., Accoroni S., Reñé A., Scardi M., Penna A. (2010). Monitoring toxic microalgae *Ostreopsis* (dinoflagellate) species in coastal waters of the Mediterranean Sea using molecular PCR-based assay combined with light microscopy. *Marine Pollution Bulletin*, 60 (7): 1074-1084.

Blackford J. C. & Gilbert F. J. (2007). pH variability and CO_2 induced acidification in the North Sea. *Journal of Marine Systems*, 64: 229-242.

Blackford J. C. & Radford P. J. (1995). A structure and methodology for marine ecosystem modelling. *Netherlands Journal of Sea Research*, 33: 247-260.

Blackford J. C. (1997). An analysis of benthic biological dynamics in a North Sea ecosystem model. *Journal of Sea Research*, 38 (3): 213-230.

Blackford J. C., Allen J. I., Gilbert F. J. (2004). Ecosystem dynamics at six contrasting sites: a generic modelling study. *Journal of marine systems*, 52 (1-4): 191-215.

Bravo I., Vila M., Casabianca S., Rodriguez F., Rial P., Riobó P., Penna A. (2012). Life cycle stages of the benthic palytoxin-producing dinoflagellate *Ostreopsis* cf. *ovata* (Dinophyceae). *Harmful Algae*, 18: 24-34.

Bratbak G. (1987). Carbon flow in an experimental microbial ecosystem. *Marine Ecology Progress Series*, 36: 267-276.

Ciminiello P., Dell'Aversano C., Fattorusso E., Forino M., Tartaglione L., Grillo C., Melchiorre N. (2008). Putative palytoxin and its new analogue, ovatoxin-a, in *Ostreopsis ovata* collected along the Ligurian coasts during the 2006 toxic outbreak. *Journal of the American Society of Mass Spectrometry*, 19: 111-120.

Ciminiello P., Dell'Aversano C., Dello Iacovo E., Fattorusso E., Forino M., Grauso L., Tartaglione L., Guerrini F., Pezzolesi L., Pistocchi R., Vanucci S. (2012[a]). Isolation and structure elucidation of ovatoxin-a, the major toxin produced by *Ostreopsis ovata*. *Journal of the American Chemical Society*, 134 (3): 1869-1875.

Ciminiello P., Dell'Aversano C., Dello Iacovo E., Fattorusso E., Forino M., Tartaglione L., Battocchi C., Crinelli R., Carloni E., Magnani M., Penna A. (2012[b]). Unique toxin profile of a Mediterranean *Ostreopsis* cf. *ovata* strain: HR LC-MS^n characterization of ovatoxin-f, a new palytoxin congener. *Chemical Research in Toxicology*, 25: 1243-1252.

Ciminiello P., Dell'Aversano C., Dello Iacovo E., Fattorusso E., Forino M., Grauso L., Tartaglione L., Guerrini F., Pistocchi R. (2010). Complex palytoxin-like profile of *Ostreopsis ovata*. Identification of four new ovatoxins by high-resolution liquid chromatography/mass spectrometry. *Rapid Communications in Mass Spectrometry*, 24: 2735-2744.

Ciminiello P., Dell'Aversano C., Dello Iacovo E., Fattorusso E., Forino M., Tartaglione L. (2011[b]). LC-MS of palytoxin and its analogues: state of the art and future perspectives. *Toxicon*, 57: 376-389.

Ciminiello P., Dell'Aversano C., Fattorusso E., Forino M., Grauso L., Tartaglione L. (2011[a]). A 4-decade-long (and still ongoing) hunt for palytoxins chemical architecture. *Toxicon*, 57: 362-367.

Ciminiello P., Dell'Aversano C., Fattorusso E., Forino M., Magno G.S., Tartaglione R., Grillo C., Melchiorre N. (2006). The Genoa 2005 outbreak. Determination of putative palytoxin in Mediterranean *Ostreopsis ovata* by a new liquid chromatography tandem mass spectrometry method. *Analytical Chemistry*, 78 (17): 6153-6159.

Cohu S., Mangialajo L., Thibaut T., Blanfuné A., Marro S., Lemée R. (2013). Proliferation of the toxic dinoflagellate *Ostreopsis* cf. *ovata* in relation to depth, biotic substrate and environmental factors in the North West Mediterranean Sea. *Harmful Algae*, 24: 32-44.

Congestri R., Bianco I., Sangiorgi V., Penna A., Zaottini E., Albertano P. (2006). *Ostreopsis Ovata* in aggregati bentonici lungo il litorale pontino. In: *101° congresso della società botanica italiana*, Caserta, 27-29 settembre 2006.

Crinelli R., Carloni E., Giacomini E., Penna A., Dominici S., Battocchi C., Ciminiello P., Dell'Aversano C., Fattorusso E., Forino M., Tartaglione L., Magnani M. (2012). Palytoxin and an *Ostreopsis* Toxin Extract Increase the Levels of mRNAs Encoding Inflammation-Related Proteins in Human Macrophages via p38 MAPK and NF-kB. *PLoS ONE*, 7 (6): e38139.

Dale B., Edwards M., Reid P. C. (2006). Phagotrophy in harmful algae. In: Granéli E., Turner J. T. (eds) *Ecology of harmful algae*. Springer, Berlin, Germany. pp. 367-378.

Del Favero G., Sosa S., Pelin M., D'Orlando E., Florio C., Lorenzon P., Poli M., Tubaro A. (2012). Sanitary problems related to the presence of *Ostreopsis* spp. in the Mediterranean Sea: a multidisciplinary scientific approach. *Annali dell'Istituto Superiore di Sanità*, 48 (4): 407-414.

Di Turi L., Lo Caputo S., Marzano M. C., Pastorelli A. M., Pompei M., Rositani L., Ungaro N. (2003). Ostropsidiaceae (Dynophyceae) presence along the coastal area of Bari. *Biologia Marina Mediterranea*, 10: 675-678.

Donovan C. J., Garduno R. A., Kalmokoff M., Ku J. C., Quilliam M. A., Gill T. A. (2009). Pseudoalteromonas bacteria are capable of degrading paralytic shellfish toxins. *Applied and Environmental Microbiology*, 75: 6919-6923.

Dubois M., Gilles K. A., Hamilton J. K., Rebers P. A., Smith F. (1956). Colorimetric method for determination of sugars and related substances. *Analytical Chemistry*, 28 (3): 350-356.

Durando P., Ansaldi F., Oreste P., Moscatelli P., Marensi L., Grillo C., Gasparini R., Icardi G. (2007). *Ostreopsis ovata* and human health: epidemiological and clinical features of respiratory syndrome outbreaks from a two year syndromic surveillance, 2005-2006, in north-west Italy. *Euro Surveillance*, 12 (23): e070607.1.

Fagerbakke K. M., Heldal M., Norland S. (1996). Content of carbon, nitrogen, oxygen, sulfur and phosphorus in native aquatic and cultured bacteria. *Aquatic Microbial Ecology*, 10: 15-27.

Faimali M., Giussani V., Piazza V., Garaventa F., Corrà C., Asnaghi V., Privitera D., Gallus L., Cattaneo-Vietti R., Mangialajo L., Chiantore M. (2011). Toxic effects of harmful benthic dinoflagellate *Ostreopsis ovata* on invertebrate and vertebrate marine organisms. *Marine Environmental Research*, 76: 97-107.

Faust M. A. & Gulledge R. A. (2002). In: *Identifying harmful marine dinoflagellates*, Smithsonian Institution, NMNH National Museum of National History, Contribution from the United States National Herbarium, 42: 1-444.

Faust M. A. (1992). Observations on the morphology and sexual reproduction of *Coolia monotis* (Dinophyceae). *Journal of Phycology*, 28: 94-104.

Faust M. A. (1998). Mixotrophy in tropical benthic dinoflagellates. In *Harmful Algae* (eds.) Reguera B., Blanco J., Fernandez M. L., Watt T.. Xunta de Galicia and IOC Commission of UNESCO, Paris, France. pp. 390-393.

Faust M. A., Morton S. L., Quod J. P. (1996). Further SEM study of marine dinoflagellates: the genus *Ostreopsis* (Dinophyceae). *Journal of Phycology*, 32: 1053-1065.

Flynn K., Francop J. M., Fernández P., Reguera B., Zapata M., Wood G., Flynn K. J. (1994). Changes in toxin content, biomass and pigments of the dinoflagellate *Alexandrium minutum* during nitrogen refeeding and growth into nitrogen and phosphorus stress. *Marine Ecology Progress Series*, 111: 99-109.

Fujiki H., Suganuma M., Nakayasu M., Hakii H., Horiuchi T., Takayama S., Sugimura T. (1986). Palytoxin is a non-12-*O*-tetradecanoylphorbol-13-acetate type tumor promoter in two-stage mouse skin carcinogenesis. *Carcinogenesis*, 7: 707-710.

Gallitelli M., Ungaro N., Addante L. M., Procacci V., Gentiloni N., Sabbà C. (2005). Respiratory illness as a reaction to tropical algal blooms occurring in a temperate climate. *Journal of the American Medical Association*, 293: 2599-2600.

Geider R. & La Roche J. (2002). Redfield revisited: variability of C:N:P in marine microalgae and its biochemical basis. *European Journal of Phycology*, 37 (1): 1-17.

Geider R. J. (1987). Light and temperature dependence of the carbon to chlorophyll a ratio in microalgae and cyanobacteria: implications for physiology and growth of phytoplankton. *New Phytologist*, 106: 1-34.

Geider R. J. (1993). Quantitative phytoplankton ecophysiology: implications for primary production and phytoplankton growth. *ICES Marine Science Symposium*, 197: 52-62

Geider R., MacIntyre H., Kana T. M. (1996). A dynamic model of photoadaptation in phytoplankton. *Limnology and Oceanography*, 41 (1): 1-15.

Geider R. J., MacIntyre H. L., Kana T. M. (1998). A dynamic regulatory model of phytoplanktonic acclimation to light, nutrients, and temperature. *Limnology and Oceanography*, 43 (4): 679-694.

Goldman J. C. (1986). On phytoplankton growth rates and particulate C: N: P ratios at low light. *Limnology and Oceanography*, 31 (6): 1358-1363.

Goldman J. C., Caron D. A., Dennet M. R. (1987). Regulation of gross growth efficiency and ammonium regeneration in bacteria by C:N ratio. *Limnology and Oceanography*, 32: 1239-1252.

Granéli E. & Hansen P. J. (2006). Allelopathy in harmful algae: a mechanism to compete for resources? In: Granéli E., Turner J. T. (eds): *Ecology of Harmful Algae*, *Ecological Studies* (189), Springer, Berlin, Germany. pp. 189-201.

Granéli E., Ferreira C. E. L., Yasumoto T., Rodrigues E. M., Neves B. (2002). Sea urchins poisoning by the benthic dinoflagellate *Ostreopsis ovata* on the Brazilian Coast. In: Steidinger K. A. (Ed.), *Xth International Conference on Harmful Algae*, vol.189. S 575 Pringer-Verlag, Heidelberg, Berlin, Germany. pp. 229-241.

Granéli E., Vidyarathna N. K., Funari E., Cumaranatunga P. R. T., Scenati R. (2011). Can increases in temperature stimulate blooms of the toxic benthic dinoflagellate *Ostreopsis ovata*? *Harmful Algae*, 10: 165-172.

Green D. H., Hart M. C., Blackburn S. I., Bolch C. J. S. (2010). Bacterial diversity of *Gymnodinium catenatum* and its relationship to dinoflagellate toxicity. *Aquatic Microbial Ecology*, 61: 73-87.

Guerrini F., Mazzotti A., Boni L., Pistocchi R. (1998). Bacterial-algal interactions in polysaccharide production. *Aquatic Microbial Ecology*, 15: 247-253.

Guerrini F., Pezzolesi L., Feller A., Riccardi M., Ciminiello P., Dell'Aversano C., Tartaglione L., Dello Iacovo E., Fattorusso E., Forino M., Pistocchi R. (2010). Comparative growth and toxin profile of cultured *Ostreopsis ovata* from the Tyrrhenian and Adriatic Seas. *Toxicon*, 55: 211-220.

Guillard R. R. L. & Ryther J. H. (1962). Studies of marine planktonic diatoms: I. *Cyclotella nana* Hustedt and *Denotula confervacea* Cleve. *Canadian Journal of Microbiology*, 8: 229-239.

Guillard R. R. L. (1975). Culture of phytoplankton for feeding marine invertebrates. In: Smith W. L. and Chanley M. H. (Eds.) *Culture of Marine Invertebrates Animals*. Plenum Press, New York, USA. pp. 26-60.

Habermann E. (1989). Palytoxin acts through Na^+/K^+-ATPase. *Toxicon*, 27: 1171-1187.

Hillebrand H. & Sommer U. (1999). The nutrient stoichiometry of benthic microalgal growth: Redfield proportions are optimal. *Limnology and Oceanography*, 44: 440-446.

Ho T. Y., Quigg A., Finkel Z. V., Milligan A. J., Wyman K., Falkowski P. G., Morel F. M. (2003). The elemental composition of some marine phytoplankton. *Journal of Phycology*, 39 (6): 1145-1159.

Honsell G., Bonifacio A., De Bortoli M., Penna A., Battocchi C., Ciminiello P., Dell'Aversano C., Fattorusso E., Sosa S., Yasumoto T., Tubaro A. (2013). New insights on cytological and metabolic features of *Ostreopsis* cf. *ovata* Fukuyo (Dinophyceae): a multidisciplinary approach. *PLoS ONE*, 8: e57291.

Hoshaw R. W. & Rosowski J. R. (1973). Methods for microscopic algae. In: Stein J. R. (Ed.), *Handbook of Phycological Methods, Culture Methods and Growth Measurements*. Cambridge University Press, Cambridge, United Kingdom. pp. 53-67.

John E. H. & Flynn K. J. (2000). Growth dynamics and toxicity of *Alexandrium fundyense* (Dinophyceae): the effect of changing N:P supply ratios on internal toxin and nutrient levels. *European Journal of Phycology*, 35 (1): 11-23.

Jürgens K., & Güde H. (1990). Incorporation and release of phosphorus by planktonic bacteria and phagotrophic flagellates. *Marine ecology progress series. Oldendorf*, 59 (3): 271-284.

Kermarec F., Dor F., Armengaud A., Charlet F., Kantin R., Sauzade D., De Haro L. (2008). Health risks related to *Ostreopsis ovata* in recreational waters. *Environmental Risques Santé*, 7: 357-363.

Klausmeier C. A., Litchman E., Daufresne T., Levin S. A. (2004). Optimal nitrogen-to-phosphorus stoichiometry of phytoplankton. *Nature*, 429 (6988): 171-174.

Legendre L. & Rassoulzadegan F. (1995). Plankton and nutrient dynamics in marine waters. *Ophelia*, 41 (1): 153-172.

Liu H. & Buskey E. J. (2000). Hypersalinity enhanced the production of extracellular polymeric substance (EPS) in the Texas brown tide alga, *Aureoumbra lagunensis* (Pelagophyceae). *Journal of Phycology*, 36: 71-77.

Louzao M. C., Ares I. R., Vieytes M. R., Valverde I., Vieites J. M., Yasumoto T., Botana L. M. (2007). The cytoskeleton, a structure that is susceptible to the toxic mechanism activated by palytoxins in human excitable cells. *FEBS Journal*, 274: 1991-2004.

Malagoli D., Casarini L., Ottaviani E. (2008). Effects of the marine toxins okadaic acid and palytoxin on mussel phagocytosis. *Fish & Shellfish Immunology*, 24: 180-186.

Mangialajo L., Bertolotto R., Cattaneo-Vietti R., Chiantore M., Grillo C., Lemée R., Melchiorre N., Moretto P., Povero P., Ruggieri N. (2008). The toxic benthic dinoflagellate *Ostreopsis ovata*: quantification of proliferation along the coastline of Genoa, Italy. *Marine Pollution Bulletin*, 56: 1209-1214.

Mangialajo L., Ganzin N., Accoroni S., Asnaghi V., Blanfuné A., Cabrini M., Cattaneo-Vietti R., Chavanon F., Chiantore M., Cohu S., Costa E., Fornasaro D., Grossel H., Marco-Miralles F., Masó M., Reñé A., Rossi A. M., Sala M. M., Thibaut T., Totti C., Vila M., Lemée R. (2011). Trends in *Ostreopsis* proliferation along the Northern Mediterranean coasts. *Toxicon*, 57: 408-420.

Menzel D. W. & Corwin N. (1965). The measurement of total phosphorus in sea water based on the liberation of organically bound fraction by persulfate oxidation. *Limnology and Oceanography*, 10: 280-282.

Monroe J. J. & Tashjian A. H. Jr. (1995). Actions of palytoxin on Na^+ and Ca^{2+} homeostasis in human osteoblast-like Saos-2 cells. *American Journal of Physiology*, 269 (C): 582-589.

Monti M., Minocci M., Beran A., Iveša L. (2007). First record of *Ostreopsis* cfr. *ovata* on macroalgae in the Northern Adriatic Sea. *Marine Pollution Bulletin*, 54: 598-601.

Moore R. E. & Scheuer P. J. (1971). Palytoxin: a new marine toxin from a coelenterate. *Science*, 172: 495-498.

Morel F. M. (1987). Kinetics of nutrient uptake and growth in phytoplankton. *Journal of Phycology*, 23 (1): 137-150.

Morton B. E., Fraser C. F., Thenawidjaja M. (1982). Potent inhibition of sperm motility by palytoxin. *Experimental Cell Research*, 140: 261-265.

Morton S. L., Norris D. R., Bomber J. W. (1992). Effect of temperature, salinity and light intensity on the growth and seasonality of toxic dinoflagellates associated with ciguatera. *Journal of Experimental Marine Biology and Ecology*, 157: 79-90.

Myklestad S. & Haug A. (1972). Production of carbohydrates by the marine diatom *Chaetoceros affinis* var. *willei* (Gran) Hustedt. I. Effect of the concentration of nutrients in the culture medium. *Journal of Experimental Marine Biology and Ecology*, 9 (2): 125-136.

Onuma Y., Satake M., Ukena T., Roux J., Chanteau S., Rasolofonirina N., Ratsimaloto M., Naoki H., Yasumoto T. (1999). Identification of putative palytoxin as the cause of clupeotoxism. *Toxicon*, 37: 55-65.

Parsons M. L. & Preskitt L. B. (2007). A survey of epiphytic dinoflagellates from the coastal waters of the island of Hawaii. *Harmful Algae*, 6: 658-669.

Pearce I., Marshall J. A., Hallegraeff G. M. (2001). Toxic epiphytic dinoflagellates from East Coast Tasmania, Australia. In: Hallegraeff G. M., Blackburn S. I., Bolch C. J., Lewis R. J. (Eds), *Harmful Algal Blooms 2000*. Intergovernmental Oceanographic Commission UNESCO, pp. 54-57.

Penna A., Bertozzini E., Battocchi C., Galluzzi L., Giacobbe M. G., Vila M., Garces E., Luglie A., Magnani M. (2007). Monitoring of HAB species in the Mediterranean Sea through molecular methods. *Journal of Plankton Research*, 29: 19-38.

Penna A., Fraga S., Battocchi C., Casabianca S., Giacobbe M. G., Riobó P., Vernesi C. (2010). A phylogeographical study of the toxic benthic dinoflagellate genus *Ostreopsis* Schmidt. *Journal of Biogeography*, 37: 830-841.

Penna A., Fraga S., Battocchi C., Casabianca S., Perini F., Cappellacci S., Casabianca A., Riobó P., Giacobbe M. G., Totti C., Accoroni S., Vila M., Reñé A., Scardi M., Aligizaki K., Nguyen-Ngoc L., Vernesi C. (2012). Genetic diversity of the genus *Ostreopsis* Schmidt: phylogeographical

considerations and molecular methodology applications for field detection in the Mediterranean Sea. *Cryptogamie, Algologie,* 33 (2): 153-163.

Penna A., Vila M., Fraga S., Giacobbe M. G., Andreoni F., Riobó P., Vernesi C. (2005). Characterization of *Ostreopsis* and *Coolia* (Dinophyceae) isolates in the western Mediterranean Sea based on morphology, toxicity and internal transcribed spacer 5.8S rDNA sequences. *Journal of Phycology,* 41: 212-225.

Perini F., Casabianca A., Battocchi C., Accoroni S., Totti C., Penna A. (2011). New approach using the real time PCR method for estimation of the toxic marine dinoflagellate *Ostreopsis* cf. *ovata* in marine environment. *PLoS ONE,* 6 (3): e17699.

Pezzolesi L., Guerrini F., Ciminiello P., Dell'Aversano C., Dello Iacovo E., Fattorusso E., Forino M., Tartaglione L., Pistocchi R. (2012). Influence of temperature and salinity on *Ostreopsis* cf. *ovata* growth and evaluation of toxin content through HR LC-MS and biological assay. *Water Research,* 46: 82-92.

Pezzolesi L., Pistocchi R., Fratangeli F., Dell'Aversano C., Dello Iacovo E., Tartaglione L.. Growth dynamics in relation to the production of the main cellular components in the toxic dinoflagellate *Ostreopsis* cf. *ovata*. *Harmful Algae,* in press.

Pfiester L. A. & Anderson D. M. (1987). Dinoflagellate reproduction. In: *The biology of dinoflagellates* (ed. F. J. R. Taylor), Blackwell, Oxford, United Kingdom. pp. 611-648.

Pin L. C., Teen L. P., Ahmad A., Usup G. (2001). Genetic Diversity of *Ostreopsis ovata* (Dinophyceae) from Malaysia. *Marine Biotechnology,* 3: 246-255.

Pistocchi R., Pezzolesi L., Guerrini F., Vanucci S. and others (2010). Influence of the environmental conditions on *Ostreopsis ovata* growth and toxicity. *Abstracts 14th Int. Conf. on Harmful Algae*, Crete, Greece, 1−5 Nov 2010. pp 48.

Pistocchi R., Pezzolesi L., Guerrini F., Vanucci S., Dell'Aversano C., Fattorusso E. (2011). A review on the effects of environmental conditions on growth and toxin production of *Ostreopsis ovata*. *Toxicon*, 57: 421-428.

Polimene L., Allen J. I., Zavatarelli M. (2006). Model of interactions between dissolved organic carbon and bacteria in marine systems. *Aquatic microbial ecology*, 43 (2), 127-138.

Polimene L., Brunet C., Butenschön M., Martinez-Vicente V., Widdicombe C., Torres R., Allen J. I. (2014). Modelling a light-driven phytoplankton succession. *Journal of Plankton Research,* 36 (1), 214-229.

Polimene L., Pinardi N., Zavatarelli M., Allen J. I., Giani M., Vichi M. (2007). A numerical simulation study of dissolved organic carbon accumulation in the northern Adriatic Sea. *Journal of Geophysical Research: Oceans (1978–2012)*, 112 (C3): C03S20.

Prandi S., Sala G. L., Bellocci M., Alessandrini A., Facci P., Bigiani A., Rossini G. P. (2011). Palytoxin induces cell lysis by priming a two-step process in MCF-7 cells. *Chemical Research in Toxicology*, 24: 1283-1296.

Ramos V. & Vasconcelos V. (2010). Palytoxin and analogs: biological and ecological effects. *Marine Drugs*, 8: 2021-2037.

Redfield A. C. (1934). On the proportions of organic derivatives in sea water and their relation to the composition of plankton. In: Daniel R. J. (ed), *James Johnstone Memorial Volume*. Liverpool University Press, Liverpool, United Kingdom. pp. 176-192.

Redfield A. C. (1958). The biological control of chemical factors in the environment. *American Scientist*, 46 (3): 205-221.

Rhodes J. A., Susuki T., Briggs L., Garthwaite I. (2000). Toxic marine epiphyte dinoflagellates, *Ostreopsis siamensis* and *Coolia monotis* (Dinophyceae) in New Zealand. *New Zealand Journal of Marine and Freshwater Research*, 33: 371-383.

Rhodes L. (2011). World-wide occurrence of the toxic dinoflagellate genus *Ostreopsis* Schmidt. *Toxicon*, 57: 400-407.

Rhodes L. L., Towers N., Briggs L., Munday R., Adamson J. (2002). Uptake of palytoxin-like compounds by shellfish fed *Ostreopsis siamensis* (Dinophyceae). *New Zealand Journal of Marine and Freshwater Research*, 36: 631-636.

Riobó P., Paz B., Franco J. M. (2006). Analysis of palytoxin-like in *Ostreopsis* cultures by liquid chromatography with precolumn derivatization and fluorescence detection. *Analytica Chimica Acta*, 66: 227-233.

Ritchie R. J. (2006). Consistent sets of spectrophotometric chlorophyll equations for acetone, methanol and ethanol solvents. *Photosynthesis Research*, 89 (1): 27-41.

Rossini G. P. & Bigiani A. (2011). Palytoxin action on the Na^+/K^+-ATPase and the disruption of ion equilibria in biological systems. *Toxicon*, 57: 429-439.

Ruardij P., Baretta J. W. , Baretta-Bekker J. G. (1995). SESAME, a Software Environment for Simulation and Analysis of Marine Ecosystems. *Netherlands Journal of Sea Research*, 33: 261-270.

Sansoni G., Borghini B., Camici G., Casotti M., Righini P., Rustighi C. (2003). Fioriture algali di *Ostreopsis ovata* (Gonyaulacales: Dinophyceae): un problema emergente. *Biologia Ambientale*, 17: 17-23.

Sechet V., Sibat M., Chomérat N., Nézan E., Grossel H., Lehebek-Peron J. B. , Jaiffrais T., Ganzin N., Marco-Miralles F., Lemée R., Amzil Z. (2012). *Ostreopsis* cf. *ovata* in the French Mediterranean coast: molecular characterization and toxin profile. *Cryptogamie Algologie*, 33: 89-98.

Shears N. T. & Ross P. M. (2009). Blooms of benthic dinoflagellates of the genus *Ostreopsis*: an increasing and ecologically important phenomenon on temperate reefs in New Zealand and worldwide. *Harmful Algae*, 8: 916-925.

Shibata A., Goto Y., Nakajima R. (2006). Use of SYBR Gold stain for enumerating bacteria and viruses in seawater samples. *Bulletin of the Plankton Society of Japan (Japan)*.

Simoni F., Gaddi A., Di Paolo C., Lepri L. (2003). Harmful epiphytic dinoflagellate on Thyrrenian Sea reefs. *Harmful Algae News*, 24: 13-14.

Simoni F., Gaddi A., Di Paolo C., Lepri L., Mancino A., Falaschi A. (2004). Further investigation on blooms of *Ostreopsis ovata, Coolia monotis, Prorocentrum lima* on the macroalgae of artificial and natural reefs in the Northern Tyrrhenian Sea. *Harmful Algae News*, 26: 5-7.

Smith G. J., Zimmerman R. C., Alberte R. S. (1992). Molecular and physiological responses of diatoms to variable levels of irradiance and nitrogen availability: growth of *Skeletonema costatum* in simulated upwelling conditions. *Limnology and Oceanography*, 37 (5): 989-1007.

Steenbergh A. K., Bodelier P. L. E., Heldal M., Slomp C. P. and Laanbroek H. J. (2013). Does microbial stoichiometry modulate eutrophication of aquatic ecosystems? *Environmental Microbiology*, 15 (5): 1572-1579.

Strickland J. D. H. & Parsons T. R. (1968). A Practical Handbook of Seawater Analysis. *Fisheries Research Board of Canada*, Bulletin 167. 311 pp.

Sun J. & Liu D. (2003). Geometric models for calculating cell biovolume and surface area for phytoplankton. *Journal of Plankton Research*, 25 (11): 1331-1346.

Taylor F. J. R. (1979). A description of the benthic dinoflagellates associated with maitotoxin and ciguatoxin, including observations on Hawaiian material. In: Taylor, D.L., Seliger, H.H. (Eds.), *Toxic Dinoflagellate Blooms*. Elsevier North Holland, New York, USA. pp. 71-76.

Tett P. & Droop M. R. (1988). Cell quota models and planktonic primary production. *Handbook of laboratory model systems for microbial ecosystems*, 2: 177-233.

Tezuka Y. (1989). The C: N: P ratio of phytoplankton determines the relative amounts of dissolved inorganic nitrogen and phosphorus released during aerobic decomposition. *Hydrobiologia*, 173 (1): 55-62.

Tichadou L., Glaizal M., Armengaud A., Grossel H., Lemée R., Kantin R., Lasalle J. L., Drouet G., Rambaud L., Malfait P., De Haro L. (2010). Health impact of unicellular algae of the *Ostreopsis* genus blooms in the Mediterranean Sea: experience of the French Mediterranean coast surveillance network from 2006 to 2009. *Clinical Toxicology*: 48, 839-844.

Tognetto L., Bellato S., Moro I., Andreoli C. (1995). Occurrence of *Ostreopsis ovata* (Dinophyceae) in the Tyrrhenian Sea during Summer 1994. *Botanica Marina*, 38 (1-6): 291-296.

Totti C., Accoroni S., Cerino F., Cucchiari E., Romagnoli T. (2010). *Ostreopsis ovata* bloom along the Conero Riviera (northern Adriatic Sea): relationships with environmental conditions and substrata. *Harmful Algae*, 9: 233-239.

Tubaro A., Durando P., Del Favero G., Ansaldi F., Icardi G., Deeds J. R., Sosa S. (2011). Case definitions for human poisonings postulated to palytoxins exposure. *Toxicon*, 57: 478-495.

Turki S. (2005). Distribution of toxic dinoflagellates along the leaves of seagrass *Posidonia oceanica* and *Cimodocea nodosa* from the gulf of Tunis. *Cahiers de Biologie Marine*, 46: 29-34.

Uemura D., Ueda K., Hirata Y., Naoki H., Iwashita T. (1981). Further studies on palytoxin. II. Structure of palytoxin. *Tetrahedron letters*, 22: 2781-2784.

Ungaro N., Marano G., Pastorelli A. M., Marzano M. C., Pompei M. (2005). In: Mattei D., Melchiorre S., Messineo V., Bruno M. (Eds) *Presenza di Ostreopsidiaceae nel basso Adriatico*, Rapporti ISTISAN 05/29. Istituto Superiore di Sanità, Roma, Italia. pp. 112-115.

Utermöhl von H. (1931). Neue Wege in der quantitativen Erfassung des Planktons. (Mit besondere Beriicksichtigung des Ultraplanktons). *Verhandlungen der lnternationalen Vereinigung für Theoretische und Angewandte Limnologie*, 5: 567-595.

Vale C. & Ares I. R. (2007). Biochemistry of palytoxins and ostreocins. In: *Botana, L.M. (Ed.), Phycotoxins, chemistry and biochemistry*. Blackwell Publishing, Ames, IA, USA. pp. 95-118.

Vanucci S., Guerrini F., Milandri A., Pistocchi R. (2010). Effects of different levels of N- and P-deficiency on cell yeld, okadaic acis, DTX-1, protein and carbohydrate dynamics in the benthic dinoflagellate *Prorocentrum lima*. *Harmful Algae*, 9: 590-599.

Vanucci S., Guerrini F., Pezzolesi L., Dell'Aversano C., Ciminiello P., Pistocchi R. (2012[a]). Cell growth and toxins' content of *Ostreopsis* cf. *ovata* in presence and absence of associated bacteria. *Cryptogamie, Algologie*, 33 (2): 105-112.

Vanucci S., Pezzolesi L., Pistocchi R., Ciminiello P., Dell'Aversano C., Dello Iacovo E., Fattorusso E., Tartaglione L., Guerrini F. (2012[b]). Nitrogen and phosphorus limitation effects on cell growth, biovolume, and toxin production in *Ostreopsis* cf. *ovata*. *Harmful Algae*, 15 (0): 78-90.

Vidyarathna N. K. & Granéli E. (2012). Influence of temperature on growth, toxicity and carbohydrate production of a Japanese *Ostreopsis ovata* strain, a toxic-bloom-forming dinoflagellate. *Aquatic Microbial Ecology*, 65: 261-270.

Vidyarathna N. K. & Granéli E. (2013). Physiological responses of *Ostreopsis ovata* to changes in N and P availability and temperature increase. *Harmful Algae*, 21-22: 54-63.

Vila M., Garcés E., Masò M. (2001). Potentially toxic epiphytic dinoflagellate assemblages on macroalgae in NW Mediterranean. *Aquatic Microbial Ecology*, 26: 51-60.

Wattenberg E. V. (2007). Palytoxin: exploiting a novel skin tumor promoter to explore signal transduction and carcinogenesis. *American Journal of Physiology. Cell Physiology*, 292 (C): 24-32.